ELSEVIER

Brain Research Bulletin, Vol. 46, No. 4, pp. 281–309, 1998

0361-9230/98 $19.00 + .00

PII S0361-9230(98)00024-0

REVIEW ARTICLE

Neurodegeneration in excitotoxicity, global cerebral ischemia, and target deprivation: A perspective on the contributions of apoptosis and necrosis

Lee J. Martin,[1,2*] Nael A. Al-Abdulla,[1] Ansgar M. Brambrink,[4] Jeffrey R. Kirsch,[3] Frederick E. Sieber[3] and Carlos Portera-Cailliau[2]

Departments of [1]Pathology, Division of Neuropathology, [2]Neuroscience, and [3]Anesthesiology/Critical Care Medicine, The Johns Hopkins University School of Medicine, Baltimore, Maryland, USA, and the [4]Department of Anesthesiology, Johannes Gutenberg-University, Mainz, Germany

[Received 16 October 1997; Revised 5 February 1998; Accepted 16 February 1998]

ABSTRACT: In the human brain and spinal cord, neurons degenerate after acute insults (e.g., stroke, cardiac arrest, trauma) and during progressive, adult-onset diseases [e.g., amyotrophic lateral sclerosis, Alzheimer's disease]. Glutamate receptor-mediated excitotoxicity has been implicated in all of these neurological conditions. Nevertheless, effective approaches to prevent or limit neuronal damage in these disorders remain elusive, primarily because of an incomplete understanding of the mechanisms of neuronal death in *in vivo* settings. Therefore, animal models of neurodegeneration are crucial for improving our understanding of the mechanisms of neuronal death. In this review, we evaluate experimental data on the general characteristics of cell death and, in particular, neuronal death in the central nervous system (CNS) following injury. We focus on the ongoing controversy of the contributions of apoptosis and necrosis in neurodegeneration and summarize new data from this laboratory on the classification of neuronal death using a variety of animal models of neurodegeneration in the immature or adult brain following excitotoxic injury, global cerebral ischemia, and axotomy/target deprivation. In these different models of brain injury, we determined whether the process of neuronal death has uniformly similar morphological characteristics or whether the features of neurodegeneration induced by different insults are distinct. We classified neurodegeneration in each of these models with respect to whether it resembles apoptosis, necrosis, or an intermediate form of cell death falling along an apoptosis-necrosis continuum. We found that *N*-methyl-D-aspartate (NMDA) receptor- and non-NMDA receptor-mediated excitotoxic injury results in neurodegeneration along an apoptosis-necrosis continuum, in which neuronal death (appearing as apoptotic, necrotic, or intermediate between the two extremes) is influenced by the degree of brain maturity and the subtype of glutamate receptor that is stimulated. Global cerebral ischemia produces neuronal death that has commonalities with excitotoxicity and target deprivation. Degeneration of selectively vulnerable populations of neurons after ischemia is morphologically nonapoptotic and is indistinguishable from NMDA receptor-mediated excitotoxic death of mature neurons. However, prominent apoptotic cell death occurs following global ischemia in neuronal groups that are interconnected with selectively vulnerable populations of neurons and also in non-neuronal cells. This apoptotic neuronal death is similar to some forms of retrograde neuronal apoptosis that occur following target deprivation. We conclude that cell death in the CNS following injury can coexist as apoptosis, necrosis, and hybrid forms along an apoptosis–necrosis continuum. These different forms of cell death have varying contributions to the neuropathology resulting from excitotoxicity, cerebral ischemia, and target deprivation/axotomy. Degeneration of different populations of cells (neurons and nonneuronal cells) may be mediated by distinct or common causal mechanisms that can temporally overlap and perhaps differ mechanistically in the rate of progression of cell death. © 1998 Elsevier Science Inc.

KEY WORDS: Axotomy, Glutamate receptor, Mitochondria, Oxidative injury, Programmed cell death.

INTRODUCTION

Cell death is a fundamental biological process that is relevant to normal histogenesis, to the steady-state kinetics of healthy adult tissues, and to the pathogenesis of tissue damage and disease [52,62,75–77,130,163]. The concept of cell death was conceived early in the history of pathology, specifically in the context of disease [188]. Now it is recognized that the death of cells (or the absence of appropriate cell death) has physiological or pathological importance. Normal physiological cell death or programmed cell death (PCD) occurs continuously in populations of cells that

* Address for correspondence: Lee J. Martin, Ph.D., Johns Hopkins University School of Medicine, Department of Pathology, Division of Neuropathology, 720 Rutland Avenue, 558 Ross Research Building, Baltimore, Maryland 21205-2196 USA. Fax: 410-955-9777; E-mail: lmartin@welchlink.welch.jhu.edu

undergo slow proliferation (e.g., liver, adrenal gland) or rapid proliferation (e.g., epithelium of intestinal crypts) [18,194], and it occurs as a normal event in the deletion of certain lymphocyte clones following an immune response [169]. Also, PCD plays a major role in the normal growth and differentiation of organ systems in vertebrates and invertebrates [52,163]. For example, in the developing nervous system large numbers (~ 50%) of sensory and spinal motor neurons die during a period of naturally occurring cell death [61,62]. This PCD is responsible for matching neuronal populations to target size, and it is thought to be largely controlled by a limiting supply of target-derived trophic factors [147], but is also controlled by afferent stimulation [25,102]. In other organs, cell death occurs during the atrophy and involution of hormone-sensitive tissues and specific cell types following hormone withdrawal, such as that occurring in the prostate [79], adrenal cortex [194], endometrium [80], and brain [175]. In pathophysiological settings, inappropriate suppression of cell death can result in cancer [18,80], and failure to control the extent of cell death can occur in acquired immunodeficiency syndrome (AIDS) [169] and in some neurodegenerative diseases of infancy and childhood, such as spinal muscular atrophy [97,161]. Other forms of pathological cell death result from hypoxic–ischemic, toxic, and thermal insults [28,38,78,130,194]. Because of the importance of cell death in human disease, it has been studied from the perspective of developmental biology, immunology, endocrinology, pathology, and neurobiology. Each group may have a somewhat different perspective on the classification of cell death, its mechanisms, and its biological importance.

CELL DEATH CLASSIFICATION

Many years ago, it was suggested that physiological cell death is very different from pathological cell death because they appear structurally different [52]. Therefore, useful categories have been invented for the classification of cell death. For the past two decades, cell death has been classified conventionally as being one of two distinct types, apoptotic or necrotic, which are believed to differ morphologically and biochemically [48,76,80,194]. Physiological cell death is generally regarded as apoptotic and is considered to be an organized PCD that is mediated by active, intrinsic mechanisms; however, exogenous modulation of apoptosis occurs [48]. In contrast, pathological (or accidental) cell death is regarded as necrotic, resulting from extrinsic insults to the cell (e.g., osmotic, thermal, toxic, traumatic) [28,38,75,130]. The process of cellular necrosis involves disruption of membrane structural and functional integrity, rapid influx of Ca^{2+} and water, and subsequently, dissolution of the cell. Therefore, cellular necrosis is induced not by stimuli intrinsic to the cell *per se* (as in PCD) but by an abrupt environmental perturbation and a departure from physiological conditions.

The disadvantage of this binary scheme lies in the difficulty of classifying cell death that appears as neither purely apoptotic nor purely necrotic, but rather as a hybrid form of cell death that may fall between the two extremes. These possible intermediate forms of cell death may occur with the degeneration of neurons, where the strict distinctions between apoptosis and necrosis are becoming less clear [24,112,152,153,178]. Other schemes for classifying cell death identify the degeneration as nuclear or cytoplasmic, depending on where the early, morphologically detectable changes occur [150]. An additional scheme for neuronal death classification is based on the finding that dying cells can display one of at least three different morphological phenotypes, designated as apoptotic, endocytic–autophagic, and nonlysosomal vesiculate [24]. Still, another variant of the nomenclature argues that the two main categories of cell death should be designated as apoptosis and oncosis (rather than apoptosis and necrosis), because both pathways of destruction ultimately lead to cellular necrosis [113]. More recently, the concept of an apoptosis–necrosis continuum for cell death was formulated based on the finding that the morphological phenotypes of excitotoxic neuronal death exist as a gradient between the two major forms of cell death (i.e., apoptosis and necrosis), independent of the deoxyribonucleic acid (DNA) fragmentation signature [152,153]. This latter scheme attempts to embrace all of the possible morphological variants of classic apoptosis and necrosis following various central nervous system (CNS) insults. Here, we also show that different forms of CNS injury can produce apoptotic and necrotic neuronal death that coexist and share some common features.

The goal of this review is to critically examine cell death structure in the CNS, specifically with regard to neuronal death in models of excitotoxicity, global cerebral ischemia, and target deprivation. These animal models of neurodegeneration are important for identifying mechanisms of neuronal death occurring in the human brain and spinal cord following acute insults (e.g., focal ischemia, global ischemia, trauma) and during chronic, progressive neurodegenerative disorders [e.g., spinal muscular atrophy, amyotrophic lateral sclerosis, Alzheimer's disease (AD)]. For example, the neostriatum in newborns and the hippocampal CA1 region in adults are highly sensitive to global cerebral ischemia (which occurs during cardiac arrest) [69,81,117,120,157]. In amyotrophic lateral sclerosis (ALS) and spinal muscular atrophy, certain groups of motor neurons degenerate [71], whereas in AD, neurodegeneration is prominent in the neocortex, hippocampus, amygdala, and basal forebrain magnocellular complex [155]. There are no effective therapies for any of these neurodegenerative abnormalities. A more complete understanding of the characteristics and mechanisms of neuronal death in the *in vivo* setting is important for the subsequent development of effective approaches to prevent or limit the neurodegeneration in acute and chronic neuropathological conditions.

MORPHOLOGICAL, BIOCHEMICAL, AND MOLECULAR SIGNATURES OF CELL DEATH

The distinction between apoptotic and necrotic cell death still relies primarily on morphological criteria, despite recent advances in the identification of molecular determinants of cell death. Regardless of the classification scheme, ultrastructure is essential for reliably categorizing cell death, but, to trained eyes, light microscopy is equally valuable [77]. A histological analysis of cell death is particularly important in model systems comprised of heterogeneous cell types, where apoptosis and necrosis may coexist. The major challenge with electron microscopic analysis of degenerating cells (or parts of dying cells) is that it requires rigorous scrutiny and accurate interpretation of static images. Apoptosis and necrosis both evolve as a sequence of structural events, but the primary mechanisms that cause either form of cell death are likely to be engaged or precipitated prior to the detection of structural changes. At present, structural alterations provide strong evidence for the type of cell death and, therefore, are more reliable than biochemical markers for classifying cell death *in vivo* (see later). The corresponding molecular mechanisms for most structural stages of cell death still need to be identified.

Morphology of Apoptosis

Apoptosis has a distinctive morphological phenotype. In most classic descriptions of apoptosis, the earliest definitive changes occur within the nucleus (Fig. 1A–H) [78,80,194]. The chromatin condenses into sharply delineated, uniformly dense masses, which appear as crescents abutting the nuclear envelope or as smooth,

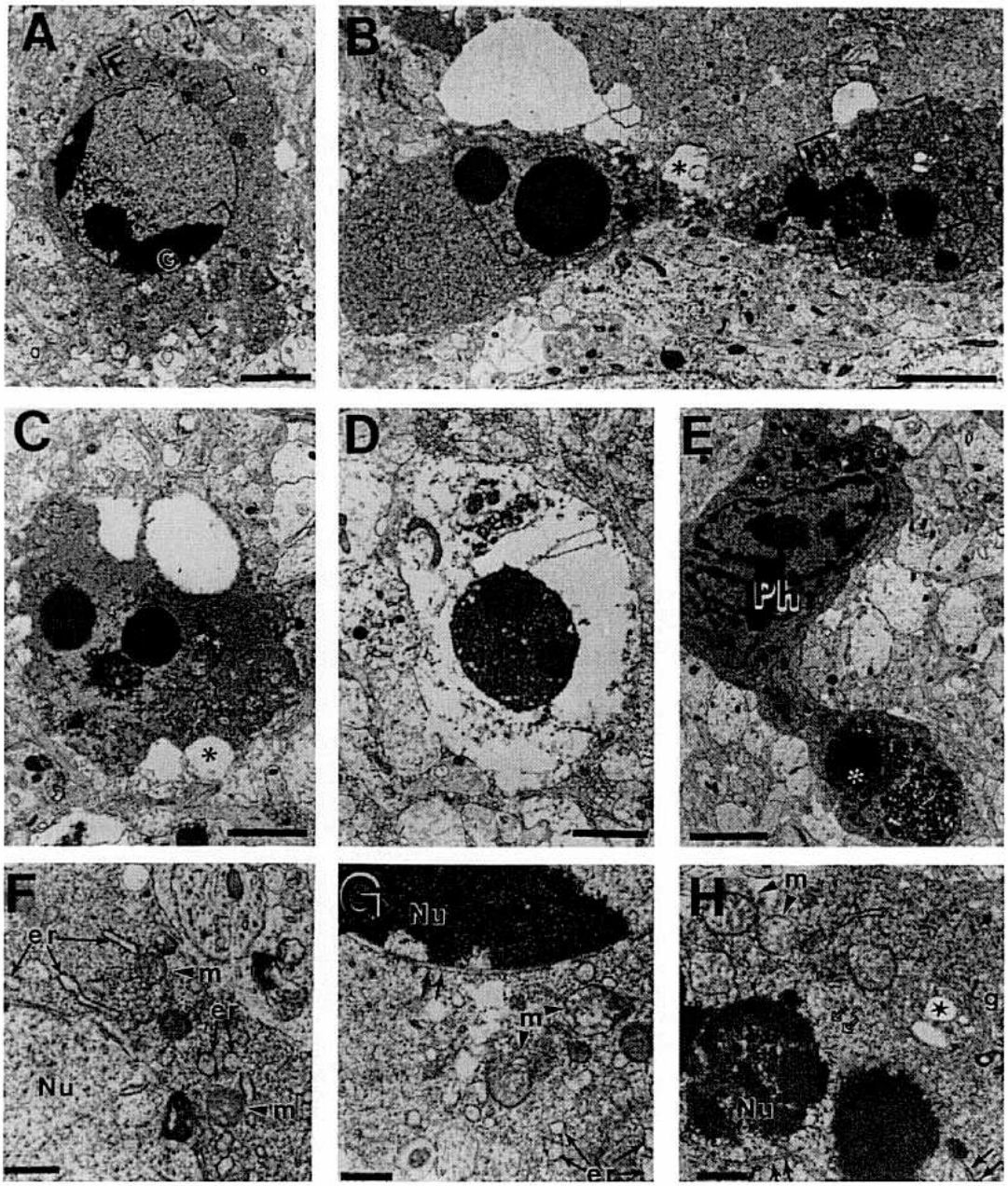

FIG. 1. Ultrastructure of apoptosis in naturally occurring cell death in developing rat brain. (A) Dying cell exhibiting early stages of apoptosis characterized by chromatin condensation as crescentic caps at the nuclear envelope as well as cytoplasmic condensation, as indicated by the homogeneously dark cytoplasm. The boxed areas are magnified in F and G to illustrate the polarity of the apoptotic process; (B) cell at later stages of apoptosis showing uniformly dense and regularly shaped, round chromatin aggregates and uniformly condensed cytoplasm. Swollen astroglial processes (asterisk) are adjacent to the dying cell. The boxed area is magnified in H; (C) apoptotic cell in advanced stages of nuclear condensation and cytoplasmic shrinkage. Swollen astroglial processes (asterisk) partially surround the dying cell; (D) apoptotic cellular debris (dark round structure) surrounded by astroglial process; (E) Cellular debris comprised of condensed cytoplasmic fragments and chromatin clumps (asterisk) is engulfed by phagocyte (Ph); (F) portion of apoptotic cell (from A) showing partially fragmented endoplasmic reticulum (er) and nearly normal mitochondria (m) within a condensed perikaryon surrounding a portion of the nucleus (Nu) without chromatin clumping; (G) another portion of an apoptotic cell (from A) showing nucleus (Nu) with chromatin crescent abutting the intact, double-membrane nuclear envelope (double arrows) and surrounding cytoplasm containing many endoplasmic reticulum-derived vacuoles (er) and swollen mitochondria (m); (H) part of a cell (from B) showing the architectural changes of late-stages of the apoptotic process. A nuclear fragment with round chromatin clumps (Nu) is surrounded by a nuclear envelope that is discernable only in some areas (solid double arrows) but not in other areas (open double arrows). The homogeneously dark, condensed cytoplasm contains swollen mitochondria (m), fragmented endoplasmic reticulum, and dilated Golgi apparatus (g, star). Electron micrographs are from postnatal day 8, rat striatum (A–C, E–H) and postnatal day 2, rat inferior colliculus (D). Scale bars: A, B, D, E, 5 μm; C, 4 μm; F–H, 1 μm. Reproduced from [153] with permission from Wiley-Liss.

round masses within the nucleus. Nucleolar disintegration also occurs early during the process of apoptosis. Activation of an endogenous endonuclease may be partly responsible for the major morphologic changes in the nucleus of thymocytes [8], but this may not be the case in other cells [143]. Prominent alterations in the cytoplasm occur concurrently with these changes in nuclear structure. The cytoplasm condenses, (as reflected by a darkening of the cell), and subsequently the cell shrinks in size, while the plasma membrane remains intact. Condensation of the cytoplasm is frequently associated with the formation of numerous, translucent cytoplasmic vacuoles [77,194]. The origin of these clear vacuoles is still uncertain, but they may be derived from the endoplasmic reticulum [75,152] or the Golgi complex [152,153]. During the course of these events, it is typically believed that the mitochondria are normal [77,78] and are required for apoptosis [89,139,198]. Subsequently, the nuclear and plasma membranes become convoluted and, then the cell undergoes a process called budding. In this process, the nucleus, containing smooth, uniform masses of condensed chromatin, undergoes fragmentation in association with the condensed cytoplasm, forming cellular debris (called apoptotic bodies) composed of pieces of nucleus surrounded by cytoplasm with closely packed and apparently intact organelles. Some nuclear fragments can be surrounded by a double membrane, whereas others are not enveloped. Apoptotic bodies are membrane-bound, and some contain well-preserved rough endoplasmic reticulum and mitochondria [77,194]. This cellular debris is then phagocytosed by nearby resident cells, typically without generating an acute inflammatory response. Therefore, infiltration of neutrophils does not occur with apoptosis, unlike that which occurs in ischemic cellular necrosis [194].

The time course for apoptosis varies in *in vitro* and *in vivo* models. Once initiated, it can be completed within 1–5 min in tumor cells cultured with cytotoxic T lymphocytes or in fibroblasts exposed to lymphotoxin [126,162]. Transforming growth factor (TGF) β1-induced apoptosis of cultured hepatocytes occurs over a 1–4 day period [142]. In an *in vitro* model of trophic factor deprivation of PC12 cells, the entire process of cell death requires approximately 1–2 days, while the apoptotic events observed morphologically occur over a 6-h period [151]. *In vivo*, the time course for apoptosis seems to depend on tissue type, occurring over a 3-h period in liver [18] and 12–18 h in adrenal cortex [194]. In an *in vivo* model of excitotoxicity in newborn brain, excitotoxic neuronal apoptosis occurs over about a 24-h period [153], whereas in an *in vivo* model of target deprivation/axotomy in adult brain, the entire process of neuronal death occurs over a 7-day period, but the apoptotic period detected morphologically occurs over an interval of 24 h or less [1]. In contrast, in an *in vivo* model of deafferentation-induced apoptosis in adult brain, rapid neuronal death occurs in less than 24 h [64].

Morphology of Necrosis

Cellular necrosis is usually elicited by a rapid departure from normal, steady-state physiology, such as that occurring with toxin exposure, hypoxia–ischemia, and trauma. Cells do not die by necrosis *per se*. The term "necrosis" conveys very little about the causal mechanisms of cell death that appears morphologically necrotic. During the process of cellular necrosis, the early, causal events of cell death are likely to occur before the morphological features of cell injury are detected [38]. In particular, perturbations in cell volume homeostasis and mitochondrial function are events that lead to cellular necrosis [28,91,92,130]. Defects in membrane permeability and ion transport proteins as well as impairments in oxidative phosphorylation and depletion of high-energy phosphates are early, causal mechanisms for cellular necrosis [38].

In contrast to the controlled, well-organized, cellular dismantling that occurs with apoptosis, the morphology of obvious cellular necrosis mirrors the apparent mechanisms for injury, such as damage/dysfunction of the plasma membrane and other organelles. This morphology is very distinct from classic apoptosis [77]. Both the nucleus and cytoplasm show ultrastructural changes, with the main features being clumping of chromatin, swelling and degeneration of organelles, destruction of membrane integrity, and eventual dissolution of the cell, with the overall configuration of the moribund cell being maintained until the very end *in vivo*. The nuclear pyknosis with condensation of chromatin into many unevenly textured, irregularly shaped clumps in cellular necrosis [77,184] sharply contrasts with the formation of few, uniformly dense and regularly shaped chromatin aggregates that occurs in apoptosis [77,78]. Furthermore, in cellular necrosis, the nuclei of dying cells do not bud to form discrete, membrane-bound fragments, as in apoptosis. These differences in the condensation of nuclear chromatin in pure apoptosis and necrosis are very diagnostic. However, between these two extremes, many morphological variants of chromatin condensation may exist (see later) [1,152,153].

During the progression of cellular necrosis, cytoplasmic organelles display structural damage. The mitochondria undergo a complex sequence of changes that includes contraction or condensation of the inner membrane and dissipation of matrical granules (C phase), inner membrane swelling and cristaeolysis (S phase), formation of flocculent aggregates, and then disintegration [183]. This evolution of mitochondrial abnormalities has been demonstrated in various forms of cellular necrosis [91,92]. Ribosomes are dispersed from the rough endoplasmic reticulum and polyribosomes disassociate, resulting in many monomeric ribosomes that are found "free" in the cytoplasm, causing the cytoplasmic matrix to appear dense and granular. The cisterns of the endoplasmic reticulum and Golgi apparatus can dilate, fragment, and vesiculate, and the plasma membrane can undergo a process called blebbing [77,91]. The molecular mechanisms for these changes in organelle structure that occur during necrotic cell death still have not been identified. Many of these subcellular changes can be found when plasma membrane function and adenosine triphosphate (ATP) synthesis are impaired [91]. In addition, oxidative damage to the cytoskeleton may have a role, particularly in the process of plasma membrane blebbing [135,136]. Some of these structural changes in various organelles are reversible, if physiological conditions are restored soon enough [3]. Because cellular necrosis results in the liberation of antigenically active, denatured intracellular debris, it is accompanied by an inflammatory response, which includes leukocytic infiltration, tissue edema, and ultimately a gross change in the overall histology of the focus of tissue damage due to the formation of a "scar."

The morphologically discernable time course for necrotic cell death is generally not dramatically different from the timing of apoptosis, once the onset is detected. *In vitro*, necrotic cell death occurs during a period of 1–2 h in disassociated fibroblast cultures [162], 1–3 h in glutamate challenged cerebellar granule cell cultures [5], and 24 h in anoxic substrate-deprived liver slices [183]. *In vivo*, excitotoxicity causes necrosis of neurons in less that 24 h [41,152,153]. Renal ischemia causes tubular epithelial cell necrosis in less than 2 days [53]. Global cerebral ischemia causes acute necrosis of principal striatal neurons in less than 24 h [119,120, 149], and degeneration of CA1 neurons 2–4 days later [69,81, 157]. In hippocampus, this neuronal death has been called postischemic "delayed neuronal death" by Kirino [81], and its classification is now controversial (see later).

A characteristic of cellular necrosis is that its rate of progression depends on the initial severity of the environmental insult

either *in vitro* or *in vivo*. In cerebral ischemia, this tenet is called "the maturation phenomenon," and it holds that the greater the severity of the ischemic insult, the more rapid is the progression of neuronal injury [69]. This general principle holds true for toxicological insults to the brain and other organs [121,122]. In contrast to cellular necrosis, no clear evidence indicates that an analogous "dose–response" principle governs the rate of progression of apoptosis *in vivo*, but rather it appears to be more of an all-or-none phenomenon.

DNA Fragmentation in Apoptosis and Necrosis

Biochemical markers have been used to classify cell death. The most extensively used biochemical signature for cell death is based on the integrity of nuclear DNA [193]. During cell death, Ca^{2+}/Mg^{2+}-activated endonucleases digest DNA [8,178,193]. Genomic DNA degradation indicates an irreversible stage of cell death. In apoptotic thymocytes, the characteristic morphological alterations in the nucleus may result from a selective nuclease activation without concurrent protease activation [8]. It is generally believed that cleavage of double-strand DNA occurs by endogenous, nonlysosomal, Ca^{2+}/Mg^{2+}-dependent endonuclease(s), specifically at regions between nucleosomes (DNA within nucleosomes is presumably not accessible to endonuclease due to packaging with histone proteins) [178], producing DNA fragments that are multiples of approximately 180 base pairs [8,193]. However, some extracellular factors [e.g., tumor necrosis factor (TNF)] can trigger DNA fragmentation during apoptosis in the absence of increases in intracellular Ca^{2+} [63]. The proteins with the endonuclease activity responsible for internulceosomal DNA cleavage have not been fully characterized. One protein has been identified (DNA fragmentation factor-45) that functions downstream of caspase-3 to cause internucleosomal DNA digestion during apoptosis [109]. In contrast with cellular necrosis, endonucleases cleave DNA less selectively (presumably because proteases are co-activated, causing digestion of histones and increased accessibility of nucleosomal DNA), producing random DNA digestion [26,178]. It is interesting in this regard that in neurons, but not in glial cells or fibroblasts, stimulated increases in intracellular Ca^{2+} are greater and occur faster in the nucleus than in the cytosol [156].

By agarose gel electrophoresis, the detection of internucleosomal DNA cleavage (the "ladder" pattern) is widely used as an indicator of apoptosis, whereas random DNA digestion (the "smear" pattern) is used as a marker for cellular necrosis [193]. However, biochemical markers of cell death vary from one cell type to another. In some cell cultures, apoptotic cell death occurs in the absence of demonstrable internucleosomal DNA fragmentation [26,143,177]. In addition, internucleosomal fragmentation occurs in ischemic liver necrosis [44] and in NMDA receptor-mediated excitotoxic neuronal necrosis in brain [152]. When using DNA fragmentation patterns as a marker to classify the type of cell death, another important consideration is the model system of cell death in which DNA integrity is being analyzed. For example, this type of analysis has definite advantages when using a homogeneous population of cells in culture, but the interpretation of similar analyses is much more difficult when performed on tissues comprised of heterogeneous cell types, such as CNS tissues with a variety of different neuronal and glial types, all of which contribute to the pool of extracted DNA. Therefore, in heterogeneous cell systems, tissue homogenization precludes the ability to evaluate cell death on a cell by cell basis. In addition, the development of inflammation with immigration of leukocytes into a region of injured tissue, and subsequent apoptosis of these cells, can complicate the interpretation of biochemical analyses of cell death produced *in vivo* [194], by adding yet another source of cellular heterogeneity and contamination. This has been recognized in cerebral ischemia [120]. Therefore, as concluded appropriately in several studies [26,77,152], ultrastructural morphology is still the best approach to classify cell death *in vivo*, providing that the electron micrographs are interpreted correctly.

The development of a technique to detect DNA fragmentation *in situ*, at the cellular level, provided a new approach to assay for cell death. This strategy is based on end-labeling single-strand or double-strand DNA breaks using DNA polymerase [54,192] or terminal deoxynucleotidyl transferase [47], respectively, to catalyze the transfer of deoxyuridine triphosphate (conjugated with a reporter molecule). The former method is called the *in situ* nick translation technique and the latter approach is called the terminal transferase-mediated dUTP nick-end labeling (TUNEL) method. Although both techniques are highly reliable for identifying cells with fragmented DNA, several questions remain unanswered. For example, does all labeling with these techniques signify ongoing or end stage cell death or perhaps DNA repair? Furthermore, a common misconception is that these methods, notably the TUNEL assay, are specific for detecting apoptotic cell death. However, these methods do not discriminate among apoptotic and necrotic cell death [54,56,152], and therefore, fail to provide insight into the mechanisms for cell death.

Molecular Mechanisms of Apoptosis

Several apoptosis-regulating genes were originally identified in the invertebrate *C. elegans*, and growing families of homologous genes that regulate apoptosis have been more recently identified in vertebrates [131,165]. One family is the group of cysteine proteases, called caspases (10 members have been identified to date), which are constitutively expressed proenzymes that undergo proteolytic cleavage and rearrangement of subunits to produce active enzymes with substrates such as nuclear proteins (e.g., polyADP-ribose polymerase, DNA-dependent protein kinases, heteronuclear ribonucleoproteins, or lamins), cytoskeletal proteins (e.g., actin, fodrin), or inflammatory mediators (e.g., prointerleukin-1β) [165]. Another group of apoptosis regulatory genes is the *bcl-2* protooncogene family [131]. Membership into the family of Bcl-2-related proteins is defined by homology domains (BH-1, BH-2, and BH-3), which function in the interactions between members. Of these genes, *bcl-2*, *bcl-x_L*, and *mcl-1* are antiapoptotic, whereas *bax*, *bcl-x_S*, *bad*, *bak*, and *bik* are proapoptotic. The complex, steady-state permutations in protein dimerization among members have a major influence on whether a cell lives or dies. For example, Bcl-2 exerts its antiapoptotic function by forming heterodimers with Bax [131].

Considerable data have accrued indicating that mitochondria participate in the critical effector stage of apoptosis. Based on early electron microscopy studies of nonneuronal cells, it has been generally believed that the ultrastructure of mitochondria remains largely intact during apoptosis [77,78]. The localization of Bcl-2 to cytoplasmic membranes that face the cytosol, including the outer mitochondrial membrane [106], further supports a role for mitochondria in apoptosis. Subsequently, it was shown that *in vitro* apoptosis in *Xenopus* egg extracts requires a dense organelle fraction enriched in mitochondria [139] and that a change in mitochondrial permeability transition constitutes an early event for nuclear apoptosis in cell-free systems [198]. A decrease in mitochondrial transmembrane potential, followed by mitochondrial uncoupling and generation of reactive oxygen species (ROS), precedes the formation of the apoptotic nuclear morphology *in vitro* [89].

Cytochrome c is a necessary component of the apoptotic program, suggesting that mitochondria participate in apoptosis by

releasing cytochrome c into the cytosol [99,108]. The liberation of cytochrome c from mitochondria may occur prior to permeability transition pore opening [86,196]. In a recently proposed model of apoptosis based on *in vitro* experiments, cytochrome c, identified as apoptotic protease activating factor-2 (Apaf-2), is a potent activator of caspases in cytosolic extracts [99]. Cytosolic ATP or deoxyadenosine triphosphate (dATP) are required cofactors for cytochrome c-induced caspase activation [99,108]. Cytochrome c and dATP bind and activate caspase-9 (Apaf-3), which in turn cleaves and activates caspase-3 [99]. Apaf-1, a yet to be fully characterized 130 kilodalton protein, serves as a docking protein for caspase-9 and cytochrome c [99]. Activated caspases cleave a protein with DNase activity (DNA fragmentation factor-45), and this cleavage activates a pathway leading to the internucleosomal fragmentation of genomic DNA [109]. In response to several apoptosis-inducing agents, cytochrome c is released from mitochondria to the cytosol [99,108] through a mechanism that may involve the formation of membrane channels comprised of Bax [6]. The antiapoptotic proteins Bcl-2 and Bcl-x_L block the release of cytochrome c from mitochondria [86,196] and therefore, the activation of caspase-3 [99,108]. The blockade of cytochrome c release from mitochondria by Bcl-2 and Bcl-x_L is possibly due to the inhibition of Bax channel-forming, proapoptotic activity in the outer mitochondrial membrane [6], or to the regulation of mitochondrial membrane potential and volume homeostasis [185].

NEURONAL DEATH IN EXCITOTOXICITY

In the CNS, neuronal death can be induced by excitotoxicity, a concept formulated by Olney that has fundamental importance to a variety of neurological disorders [110,145,146]. This pathologic neurodegeneration is mediated by excessive activation of glutamate-gated ion channel receptors and probably voltage-dependent ion channels as well. The precise mechanisms of excitotoxic cell death are unclear, and both *in vitro* and *in vivo* data are discordant with regard to whether excitotoxic neuronal death is apoptotic or necrotic. The excessive interaction of ligand with subtypes of glutamate receptors alters intracellular ion concentrations, pH, protein phosphorylation, and energy metabolism [22,105,190]. An increase in cytosolic free Ca^{2+} causes and activation in Ca^{2+}-sensitive proteases, protein kinases/phosphatases, and phospholipases when glutamate receptors are stimulated. Likewise, excitotoxicity results in an activation of endonucleases and subsequent internucleosomal DNA fragmentation in cultures of cortical neurons [59,90] and cerebellar granule cells [5,174], although others have not found internucleosomal DNA fragmentation in cerebellar granule cell cultures [33]. This excitotoxin-induced cell death *in vitro* has been shown to be prevented [90] or unaffected [33,59, 174] by inhibitors of ribonucleic acid (RNA) or protein synthesis and is either sensitive [90,174] or insensitive [33] to the endonuclease inhibitor aurintricarboxylic acid. An internucleosomal pattern of genomic DNA fragmentation has also been observed *in vivo* 12–48 h after intracerebral injections of excitotoxins [41,152, 153,186], and this pattern can persist to 5 days postlesion [186].

The *in vivo* morphological characteristics of excitotoxicity in many neurons include somatodendritic swelling, chromatin condensation into irregular clumps, and organelle damage [145,146,152,153, 186], features that are thought to be typical of cellular necrosis [77,78,194]. However, in other neurons, excitotoxicity causes cytological features more reminiscent of apoptosis [153,186]. Excitotoxic neurodegeneration *in vivo* has been shown to be either sensitive [164] or insensitive [98] to protein synthesis inhibition; therefore, a role for *de novo* protein synthesis in the expression of a PCD cascade in excitotoxicity is uncertain.

Excitotoxic Neuronal Death is Influenced by Brain Maturity and Glutamate Receptor Subtype Stimulation: The Apoptosis–Necrosis Morphological Continuum

We tested the hypothesis that glutamate receptor-mediated excitotoxicity *in vivo* induces neuronal death with phenotypes that vary depending on the maturity of the brain at the time of the insult and on the glutamate receptor subtype that is activated. As a logical prelude to these experiments, we characterized normal developmental cell death in the newborn brain with respect to DNA fragmentation patterns and ultrastructure to establish a standard for apoptosis in the CNS [153], against which we could compare induced neuronal death. In developing rat brain, normal physiological neuronal death is associated with internucleosomal fragmentation of DNA [153], and its ultrastructure (Fig. 1A–H) is similar to neuronal apoptosis described in developing chick ciliary ganglion [150] and spinal cord [23,141] and in nonneuronal systems [76,80,167]. Although it is difficult to construct a temporal sequence of developmental neuronal death, this neurodegeneration is characterized by chromatin condensation into crescentic caps abutting the nuclear envelope or into few uniform round clumps and by an increased nuclear and cytoplasmic matrix density, as reflected by a darkening of the cell (Fig. 1A–H). The increased cytoplasmic matrix density appears to be related to a disaggregation of polyribosomes into monosomes, a breakdown of the rough endoplasmic reticulum into smaller tubular and round fragments, and a disappearance of Golgi stacks. At later stages of developmental neuronal apoptosis, the nuclear envelope becomes less distinct and the mitochondria swell and disintegrate. Ultimately, the dying neuron undergoes fragmentation, and cellular debris, often appearing secondarily necrotic, is engulfed by nonneuronal cells (Fig. 1A–H).

In the newborn rat brain, excitotoxic activation of NMDA and non-NMDA glutamate receptors causes neuronal death with phenotypes ranging from apoptosis to necrosis [153]. At first glance, three structurally different forms of dying cells can be identified (Fig. 2A–C): a classic apoptotic form; a vacuolated form, similar to the endocytic-autophagic type described by Clarke and coworkers [24,68]; and a classic necrotic form. When we evaluated the progression of excitotoxin-induced, neuronal apoptotic death in the newborn brain, we found that the vacuolated form is a precursor stage of apoptosis, which has many similarities to PCD occurring in the developing brain (Fig. 3A–L) [153].

In contrast, in the adult rat brain, excitotoxic neuronal death caused by NMDA receptor activation is morphologically necrotic (Fig. 4A–J) [152]. However, neuronal death produced by non-NMDA receptor activation is distinct from that caused by NMDA receptor stimulation (Figs. 4A–I and 5A–I). Non-NMDA receptor-mediated neuronal death in adult brain has some cytoplasmic and nuclear features reminiscent of neuronal apoptosis in the excitotoxically injured newborn brain (Figs. 3A–L and 5A–I), although non-NMDA receptor excitotoxic neurodegeneration in adult brain and naturally occurring apoptosis in developing brain are very different structurally (Figs. 1A–H and 5A–I).

Excitotoxically injured neurons die with morphologic changes that are characterized by a highly ordered sequence of organelle abnormalities (Fig. 6A–F). The sequential subcellular changes that occur during excitotoxic neuronal death are rough endoplasmic reticulum dilatation, polyribosomal disaggregation, Golgi vesiculation, and then mitochondrial swelling as well as chromatin condensation (Fig. 6A–F). However, excitotoxicity in adult brain caused by both NMDA and non-NMDA receptors is associated with internucleosomal DNA fragmentation [152], despite the definite absence of a classic apoptotic morphological phenotype in dying neurons.

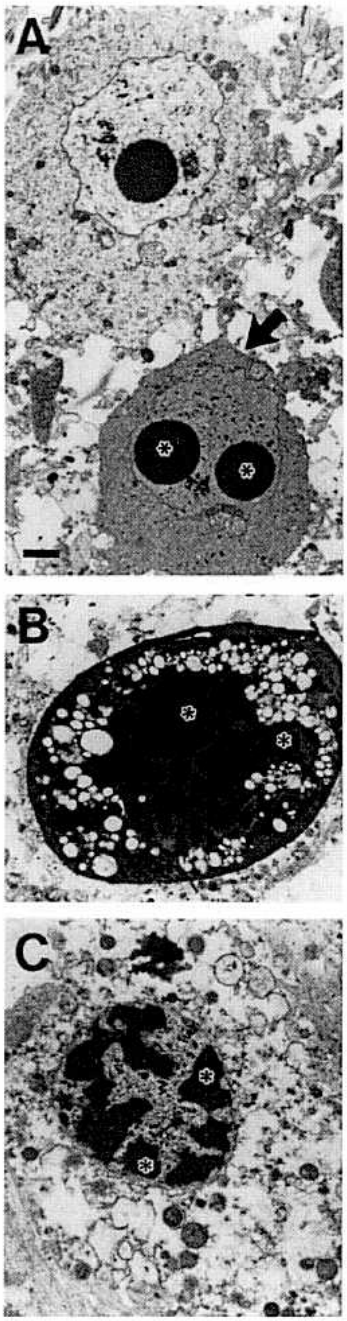

FIG. 2. Kainic acid-induced excitotoxicity in newborn rat (postnatal day 5) cerebral cortex (20 h postinjection) causes cell death ranging from classic apoptosis to classic necrosis. (A) Electron micrograph of dying cell in layer VI undergoing classic apoptosis (arrow). The nucleus contains large, dark, round clumps of chromatin (asterisks) and is surrounded by an intact nuclear envelope. The cytoplasm is homogeneously dark and condensed (see Fig. 1B,C); (B) electron micrograph of a dying cell in layer V with a vacuolated phenotype. The dark, pyknotic nucleus contains many, irregularly-shaped clumps of chromatin (asterisks). The dark cytoplasm contains many vacuoles. Both the nuclear envelope and plasma membrane are intact; (C) electron micrograph of a dying cell (located in a superficial layer) with a classic necrotic phenotype. The overall configuration of the cell is maintained, but the nucleus contains several, irregularly-shaped aggregates of chromatin (asterisks), rather than discrete round clumps, and the cytoplasm shows severe dissolution and loss of membrane integrity. Scale bar: A, 4 μm (same for B and C).

Excitotoxic Neurodegeneration: Conclusions

Our experiments comparing naturally occurring neuronal death and excitotoxic neuronal death in the developing and adult CNS led to the concept of an apoptosis–necrosis continuum for neuronal death *in vivo*. We conclude that excitotoxic neurodegeneration does not have to be strictly apoptotic or necrotic, according to a traditional binary classification of cell death, but can exist as intermediate or hybrid forms of cell death that lie along a structural continuum with apoptosis and necrosis at the extremes. This continuum is influenced by the subtype of glutamate receptor that is activated; therefore, excitotoxic neuronal death is not identical in every neuron [152,153], possibly because of the high diversity in the expression, localization, and function of glutamate receptor subtypes and second messenger systems [42,72,114–116]. We also conclude that the structure of neuronal death is influenced by CNS maturity, because death of injured adult neurons only rarely occurs with *bona fide* apoptotic morphological features [1,64,175] that closely resemble those seen during naturally occurring cell death in the developing nervous system [23,24,141,150,153,167].

NEURONAL DEATH IN CEREBRAL ISCHEMIA

The mechanisms by which transient cerebral ischemia produces irreversible neuronal death are still not fully understood and are now even more obscured by attempts to explore the contribution of PCD to ischemic neurodegeneration. The finding that degeneration of CA1 pyramidal neurons is delayed following transient forebrain ischemia [69,81,157] is appealing in the context of a possible role of PCD in this neurodegeneration. The underlying assumption is that some active cell death mechanism is engaged during the temporal delay between the initial insult and the ultimate degeneration of CA1 neurons. It is important to recognize, however, that the "delay" in the postischemic degeneration of CA1 pyramidal neurons is relative and can be truncated depending on the principle of the maturation phenomenon [69]; therefore, CA1 neurodegeneration can evolve more rapidly, depending on the severity of the insult.

The initial suggestion that postischemic delayed neuronal death in hippocampus had some possible relationship to PCD was based on the finding that systemic treatment with protein synthesis inhibitors (cycloheximide or anisomycin) protected against CA1 neuron loss in rat [55] and gerbil [170]. It is still uncertain whether this protection reflects a persistent suppression of neuronal death or an extended delay of neurodegeneration. However, a subsequent study showed that neither protein synthesis inhibitors (anisomycin and cycloheximide) nor an RNA synthesis inhibitor (actinomycin D) protected against postischemic delayed neuronal death in rat CA1 [32]. This latter study also showed by electron microscopy that delayed death of selectively vulnerable neurons does not have the characteristics of apoptosis [32]. Our data also demonstrate that the degeneration of selectively vulnerable neurons following global ischemia is not apoptotic (Figs. 7A–F, 8A–H, 9A–J, 10A–I, 11A–I). This conclusion is based on the absence of an apoptotic morphological phenotype in these neurons and is consistent with the observation that organelles that function in protein synthesis and posttranslational modification become structurally abnormal early in the course of ischemic neurodegeneration and are persistently abnormal during the process of neuronal death [82]. These morphological changes are consistent with the finding that total protein synthesis is severely reduced by 6 h following transient global forebrain ischemia and that this robust reduction occurs persistently in CA1 neurons, with the vast majority of pyramidal neurons never regaining their normal biosynthetic activity [7,45, 73,176]. However, this finding does not completely rule out the possibility that some proteins could be translated postischemia.

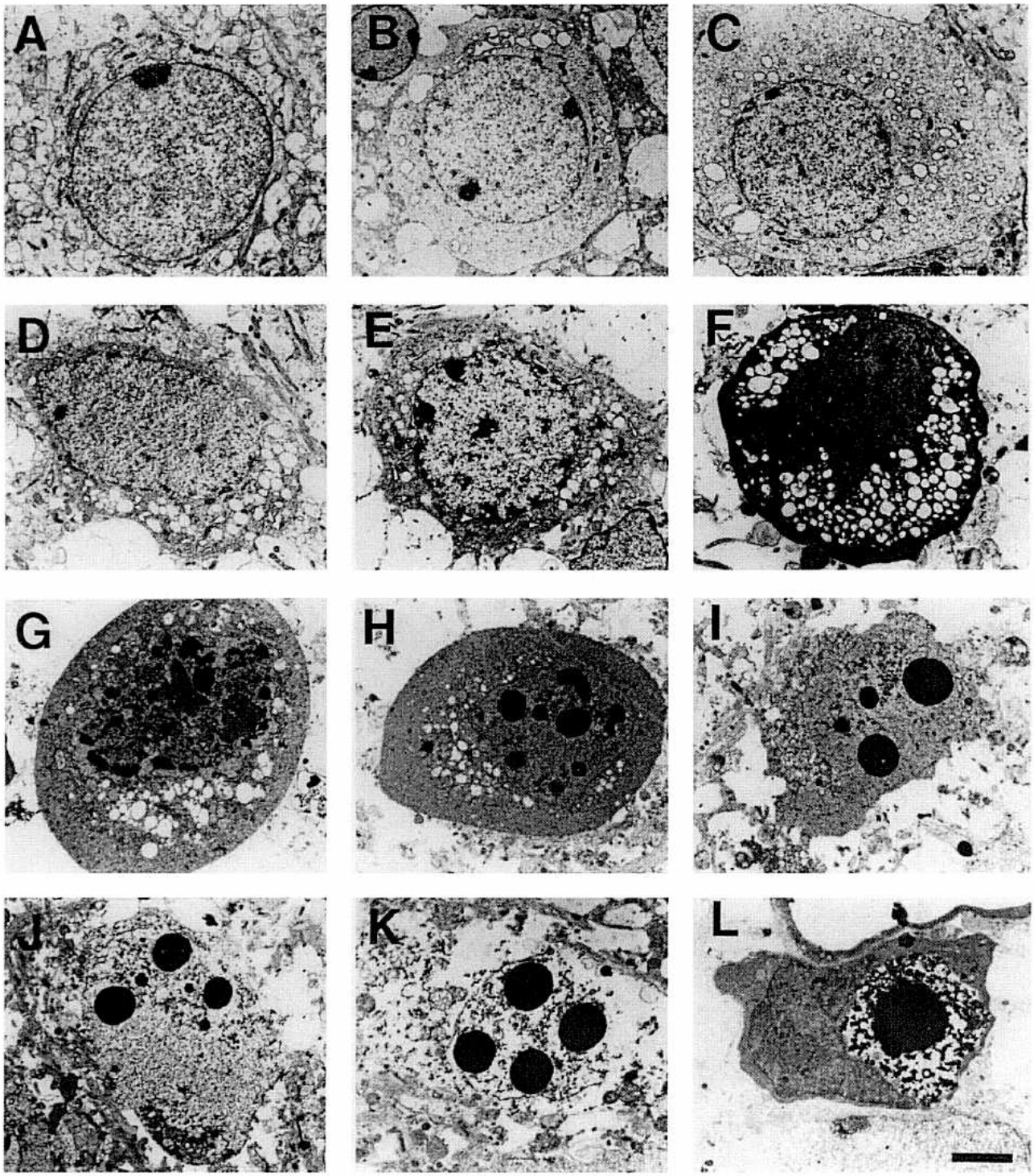

FIG. 3. Ultrastructural progression of non-NMDA receptor-mediated excitotoxic neuronal death in postnatal day 5 rat cerebral cortex caused by kainic acid. This neurodegeneration appears as a hybrid of apoptosis and necrosis, but more closely resembles apoptosis. A normal neuron (A) is shown for comparison with neurons at 15 min (B); 2 h (C); 6 h (D–F); 20 h (G–I); and 24 h (J–L) after excitotoxin injection. The temporal progression shown here has some leeway with respect to the timing of the different stages of degeneration; for example, cells shown here with a morphology at 20 h can be found at 6 h and vice versa. Vacuolation of the cytoplasm is present within 15 min (B) and increases progressively in severity over the next 6 h (C–F). At about 6 h, the chromatin begins to condense within the nucleus (E); and subsequently over the next 14 h the chromatin is condensed into large, round clumps (F–I). During this phase, the dying cell undergoes progressive cytoplasmic condensation and assumes a round morphology and then shrinks (E–I). The condensed, shrunken cell then looses plasma membrane integrity, and cytoplasmic fragments with round chromatin clumps are dispersed into the neuropil (J,K); phagocytic cells then engulf the cellular debris (L). Scale bar: L, 5 μm (same for A–K). Reproduced from [153] with permission from Wiley-Liss.

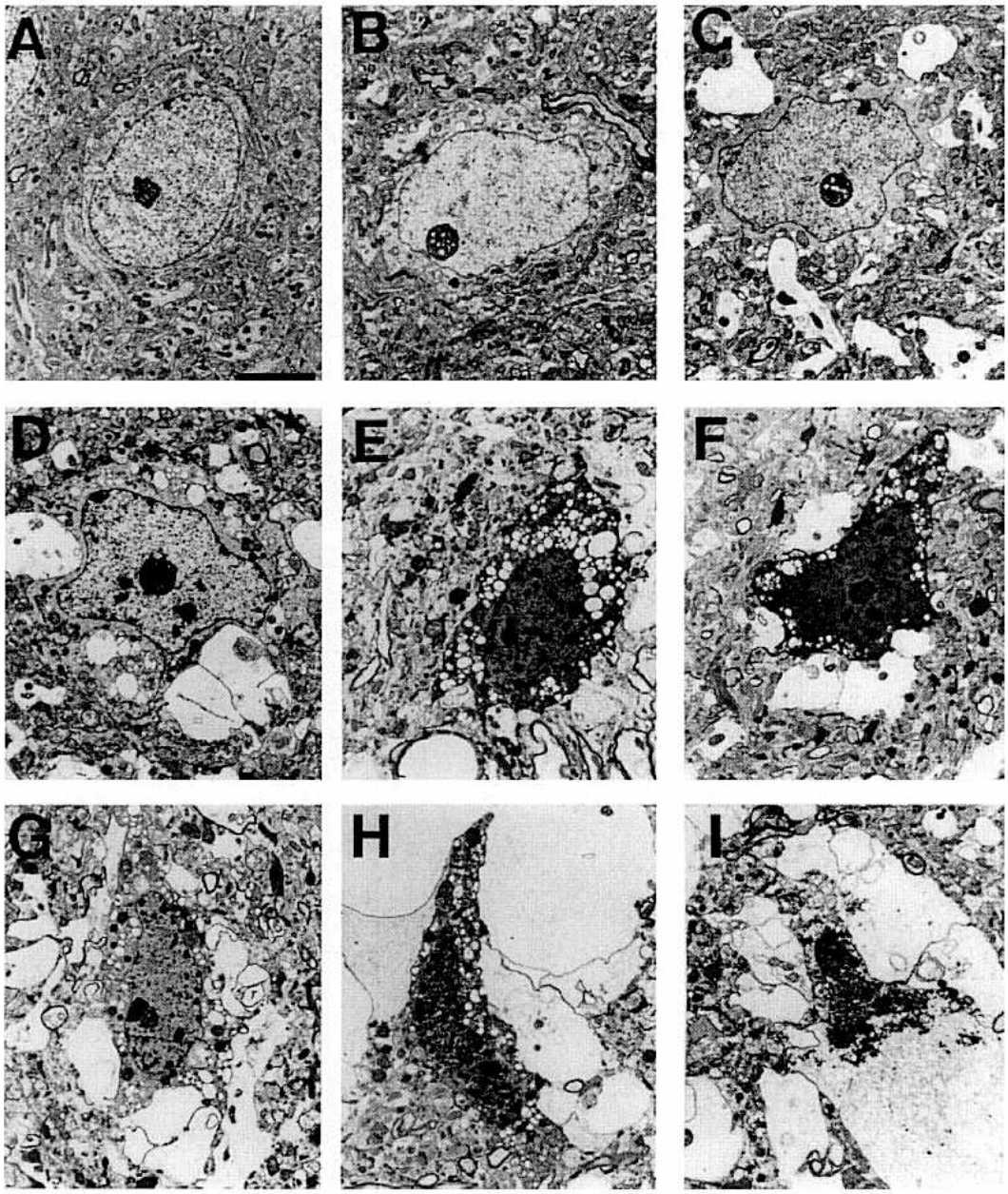

FIG. 4. Ultrastructural progression of NMDA receptor-mediated excitotoxic neuronal death in the adult rat striatum caused by quinolinic acid. This neurodegeneration is morphologically necrotic. A normal principal striatal neuron (A) is shown for comparison with neurons at 15 min and 2, 6, 12, and 24 h after excitotoxin (B–I) arranged in a temporal sequence to show the predominant structural changes associated with NMDA receptor-mediated excitotoxic neuronal necrosis. This neuronal death is not precisely synchronized because at any time point postlesion dying neurons are found at different stages of degeneration. Accumulation of cytoplasmic vacuoles occurs by 15 min after injury (B), increasing progressively during the subsequent 6 h (C–E). During this early 6-h interval (B–E), the arrays of rough endoplasmic reticulum become fragmented and many mitochondria become swollen and vacuolated, as the cytoplasmic matrix becomes progressively dark and homogeneously granular while cell becomes shrunken and the contour becomes angular. Concurrently, the nucleus shows condensation of chromatin into numerous, irregular clumps as the nuclear matrix progressively becomes uniformly dark (B–F), although the nucleolus still remains prominent until ultimate cellular disintegration. From 12–24 h, injured cells undergo dissolution as the dark, severely, vacuolated cytoplasm becomes disrupted, containing few discernible, but very swollen mitochondria, while the nucleus progressively becomes more pyknotic and undergoes karyolysis (G–I). Scale bar: A, 4 μm (same for B–I). Reproduced from [152] with permission from Wiley-Liss.

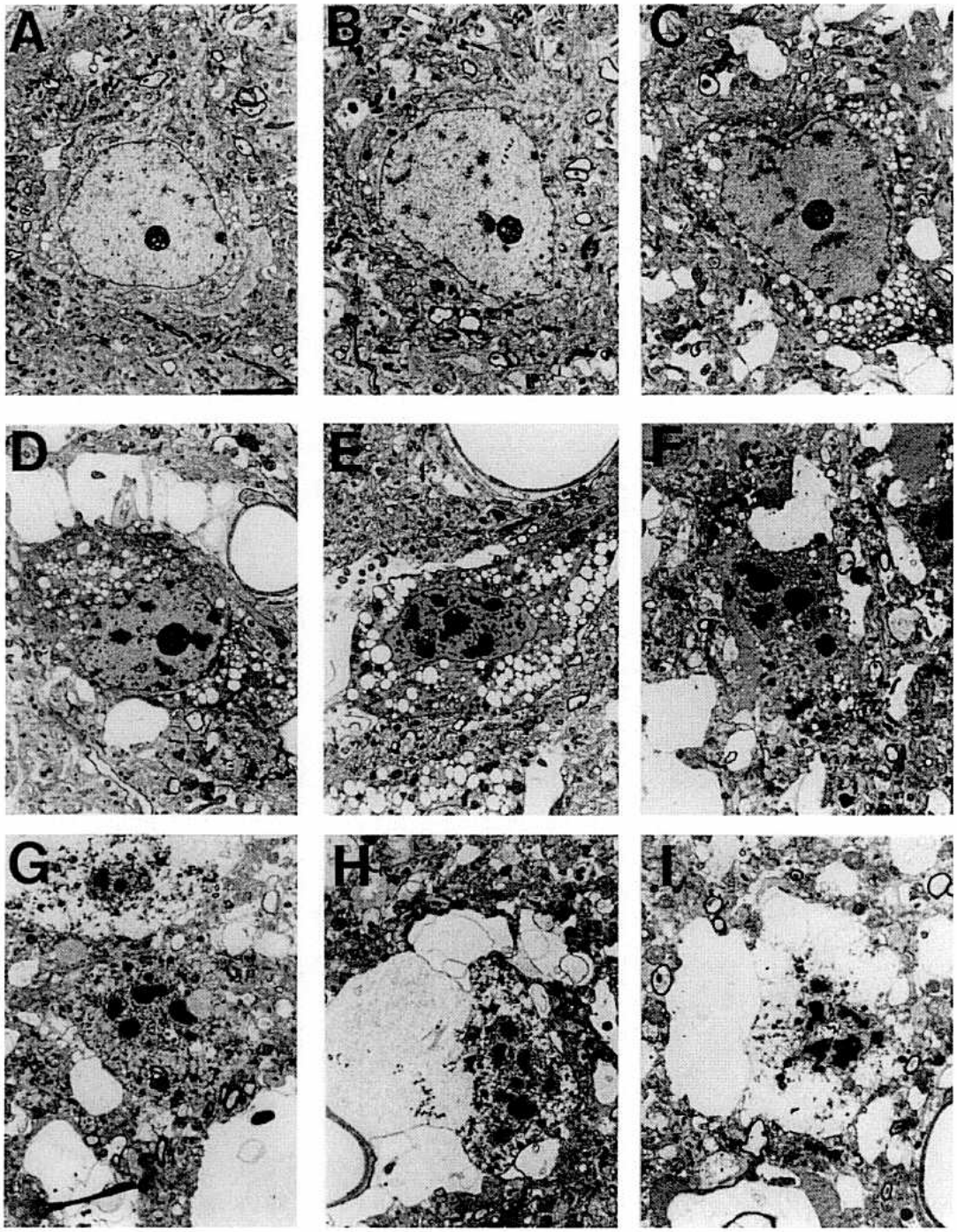

FIG. 5. Ultrastructural progression of non-NMDA receptor-mediated excitotoxic neuronal death in the adult rat striatum caused by kainic acid. This neurodegeneration has a morphological pattern that falls between classic apoptosis (see Figs. 1 and 3) and classic necrosis (see Fig. 4). Principal striatal neurons at 15 min and 2, 6, 12, and 24 h after excitotoxin (A–I) are arranged in a temporal sequence to show the predominant structural changes associated with non-NMDA receptor-mediated excitotoxicity. This neuronal death was also not precisely synchronized because at any time point postlesion there are dying neurons at different stages of degeneration. The pattern of cytoplasmic changes induced by non-NMDA receptor toxicity at 15 min (A,B) to 6 h (C–F) generally paralleled those caused by NMDA receptor toxicity (see Fig. 4), notably the severe vacuolation. Prominent differences in the progression of nuclear changes are discernible when non-NMDA receptor toxicity is compared to NMDA receptor toxicity. Over 6–12 h postlesion (D–F), kainic acid-injured neurons undergo progressive compaction of chromatin into few, discrete, large clumps, contrasting with the formation of numerous, smaller, irregular chromatin clumps observed in quinolinic acid toxicity (see Fig. 4). However, the ultimate progression of cellular dissolution (G–I) is similar with the two different excitotoxins. Scale bar: A, 4 μm (same for B–I). Reproduced from [152] with permission from Wiley-Liss.

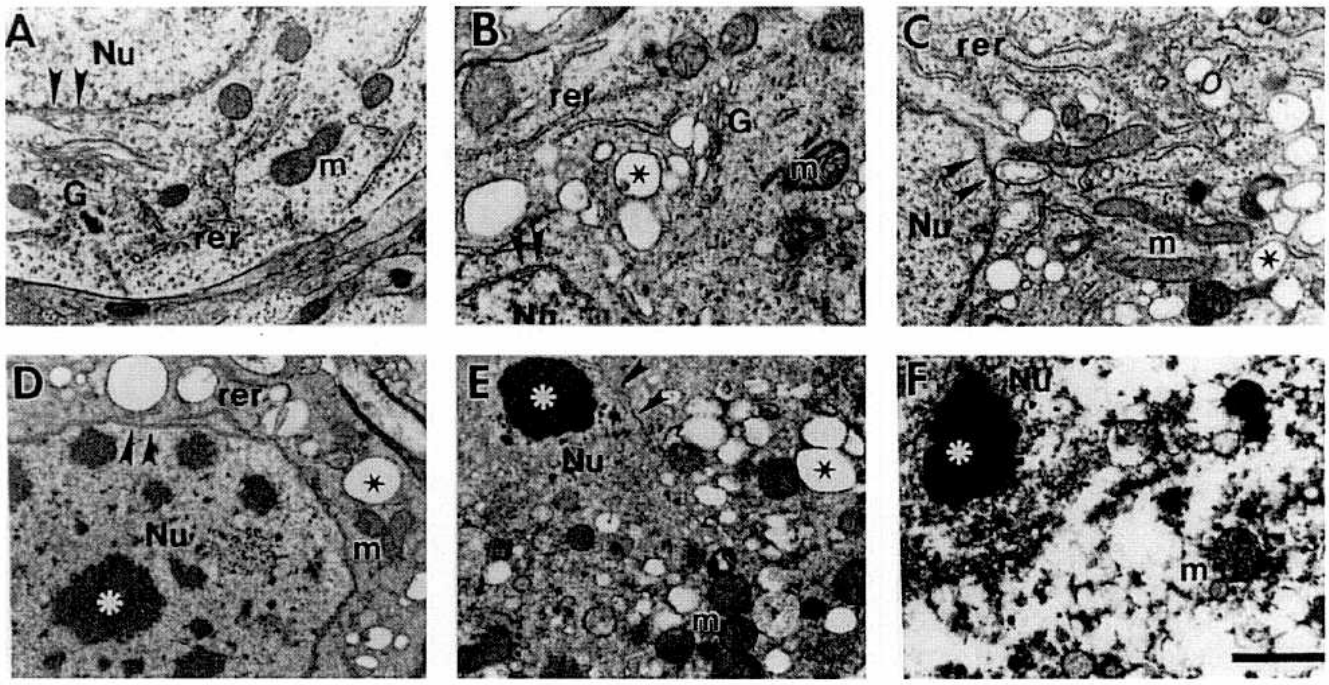

FIG. 6. NMDA and non-NMDA receptor-mediated excitotoxic death of neurons in adult rat striatum is associated with sequential and progressive subcellular abnormalities within cytoplasmic organelles. Abbreviations: G, Golgi apparatus; m, mitochondria; Nu, nucleus; rer, rough endoplasmic reticulum. The nuclear envelope is identified by the double arrowheads. (A) Normal, principal, striatal neuron with abundant polyribosomes, intact arrays of rough endoplasmic reticulum and Golgi, and normal mitochondria; (B) by 15 min after excitotoxin exposure, the Golgi swells and undergoes vesiculation to form clear vacuoles (star) and the inner mitochondrial membrane swells. The rough endoplasmic reticulum appears normal, but some free ribosomes are dispersed in the cytoplasm causing the matrix to become darker and granular; (C) by 2 h after excitotoxin exposure, many Golgi-derived vacuoles accumulate in the cytoplasm (star); (D) by 12 h after excitotoxin exposure, the cytoplasmic matrix becomes homogeneously dark and polyribosomes are no longer discernible. Numerous, Golgi-derived vacuoles of various sizes (star) are formed within the cytoplasm. The rough endoplasmic reticulum is disorganized and partially fragmented. Some mitochondria are normal but others are damaged. The nuclear chromatin undergoes condensation into clumps of various sizes (asterisk), while the nuclear envelope remains intact; (E) By 24 h after excitotoxin exposure, the cytoplasmic matrix is very dark, disorganized, and condensed. The rough endoplasmic reticulum is not discernible, and mitochondria are at various stages of degeneration. The nucleus, which contains chromatin clumps (asterisk), is no longer surrounded by an intact nuclear membrane; (F) dissolution of the neuron is associated with dispersal of dark, denatured, cytoplasmic debris and nuclear debris with chromatin clumps (asterisk). Scale bar: F, 1 μm (same for A–E). Reproduced from [152] with permission from Wiley-Liss.

Cytoskeletal damage also occurs early postischemia, particularly in dendrites, before the degeneration of neuronal cell bodies [85, 195]; this early disassembly and proteolysis of the cytoskeleton following ischemia [85] and excitotoxicity [173] contrasts with the organized appearance of the cytoskeleton in neuronal apoptosis [1].

Despite this evidence, recent studies have now attempted to reassert that delayed neuronal death of CA1 pyramidal neurons after ischemia is apoptosis [140], but convincing ultrastructural data to support this conclusion have not been forthcoming. Other groups have reported that neuronal apoptosis also occurs in newborn piglet neocortex following global hypoxia–ischemia [128] and in adult rat striatum following focal ischemia [100]. Yet, there is a paucity of ultrastructural data to support these conclusions. These recent reports are hard to reconcile with many earlier and very thorough ultrastructural studies that document that ischemic neurodegeneration in selectively vulnerable regions does not have a morphological phenotype consistent with apoptosis (although not necessarily stated explicitly in some studies, the micrographs illustrate the point) [16,32,81–83,149]. Instead, these reports demonstrate that ischemic neurodegeneration has the typical features of cellular necrosis, consistent with the acute parenchymal cell death found in other organs following ischemia [194].

Degeneration of Selectively Vulnerable Neurons After Global Ischemia Is Not Morphologically Apoptosis

Here, we have classified postischemic neurodegeneration using models of complete global ischemia in adult cat [84], incomplete global ischemia in adult dog [171,172], and global hypoxia-ischemia in newborn piglet [117–120]. The degeneration of pyramidal neurons in neocortex and CA1 (Fig. 7A–F) and of cerebellar Purkinje cells (Fig. 8A–H) in adult brain following global ischemia is not morphologically apoptosis. In our model of asphyxic cardiac arrest in piglets, the vast majority of striatal neuronal death is nonapoptotic as well (Figs. 9A–I, 10A–I, 11A–I). Like the death of CA1 pyramidal neurons after ischemia (Fig. 7A–F), the degeneration of Purkinje cells (Fig. 8A–H) and principal striatal neurons (Figs. 10A–I and 11A–I) evolves in association with damage to organelles that function in protein synthesis, posttranslational modification, and secretion. Disaggregation of polyribosomes and fragmentation or vesiculation of the endoplasmic reticulum and Golgi complex are prominent examples of this subcellular pathology that would likely alter protein synthesis/processing capabilities. The ischemic neuronal death of neocortical pyramidal neurons, CA1 pyramidal neurons, principal striatal neurons, and Purkinje cells is similar morphologically, regardless of the severity

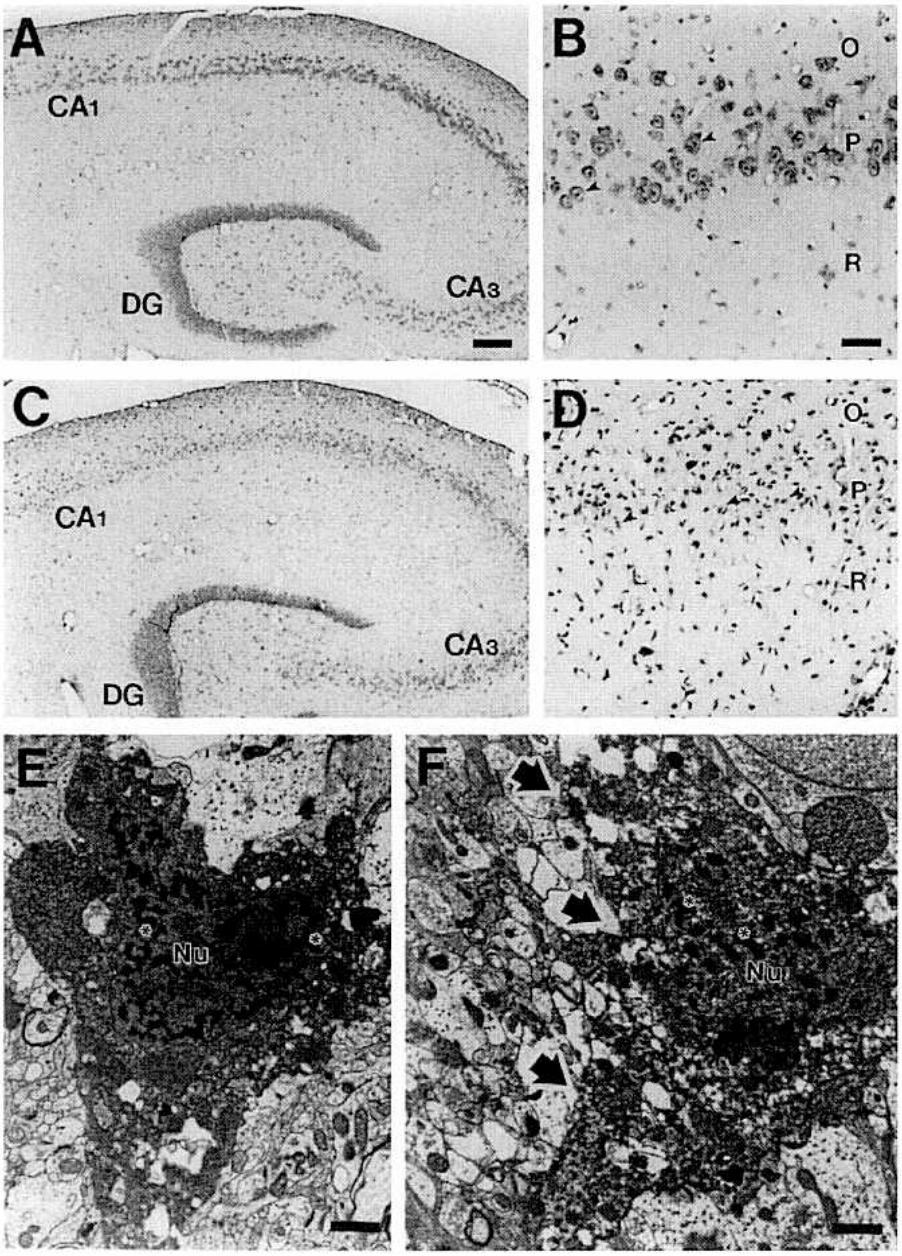

FIG. 7. Degeneration of CA1 neurons is not morphologically apoptotic following transient global ischemia. Adult cats were subjected to 10 min of ischemia, induced by temporary ligation of the left subclavian and brachiocephalic arteries plus hemorrhagic hypotension, followed by 3 days recovery. (A and B) Dorsal hippocampus of control cat showing CA1, CA3, and dentate gyrus (DG) at low magnification (A) and CA1 neurons (arrowheads) at higher magnification (B). Abbreviations: O, stratum oriens; P, stratum pyramidale; R, stratum radiatum. (C) Dorsal hippocampus of ischemic cat showing the selective vulnerability of CA1; (D) prominent degeneration of CA1 neurons (arrowheads) after ischemia. Note the severe inflammatory response typical of ischemic necrosis, as indicated by accumulation of cells with small, dark nuclei; (E) electron micrograph of a degenerated CA1 pyramidal neuron showing an ultrastructure that is not consistent with apoptosis (compare with Figs. 1, 2A, 3). The cytoplasm of the neuron contains degenerating mitochondria, and the pyknotic nucleus (Nu) contains peripherally located, irregular condensation of chromatin (asterisks); (F) Electron micrograph showing end-stage necrotic degeneration of a CA1 pyramidal neuron induced by ischemia. This neuron is undergoing dissolution of both the cytoplasm and nucleus (Nu). The nucleus contains many small aggregates of chromatin (asterisks) and is not surrounded by an intact nuclear envelope. The plasma membrane has lost integrity (arrowheads) and cellular contents are being liberated into the surrounding neuropil, consistent with the presence of an inflammatory response (see D). The ultrastructure of this delayed neuronal degeneration following ischemia is identical to that caused by NMDA-receptor mediated excitotoxicity (compare with Fig. 4). Scale bars: A, 180 μm (same for C); B, 40 μm (same for D); E, 1.2 μm; F, 0.8 μm.

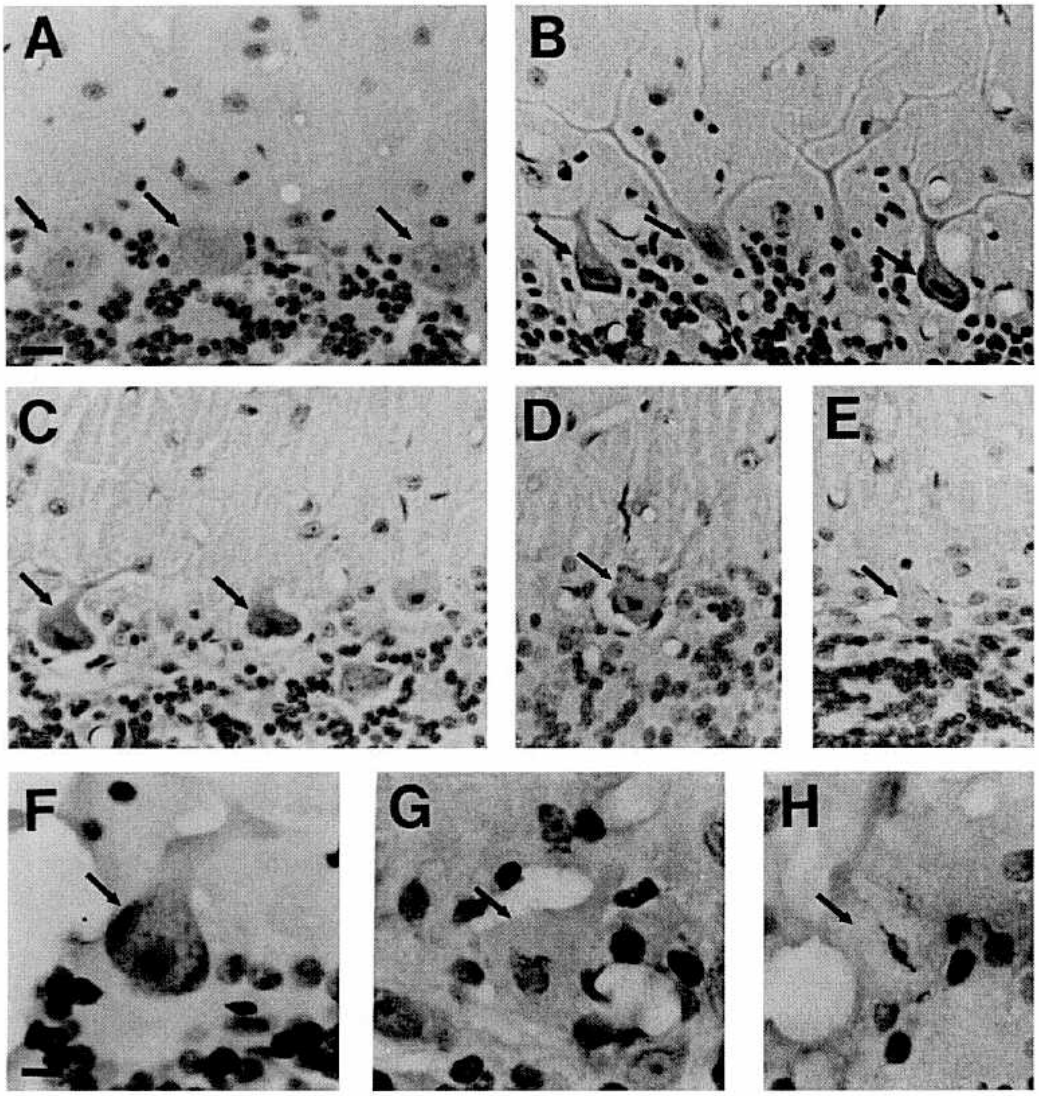

FIG. 8. Purkinje cell degeneration in cerebellum is not morphologically apoptotic following transient global ischemia. Adult cats were subjected to 10 min of ischemia, induced by temporary ligation of the left subclavian and brachiocephalic arteries plus hemorrhagic hypotension, followed by 3 days recovery. Because different cerebellar folia show varying vulnerabilities to ischemia and Purkinje cell death is not synchronous, a four-stage temporal morphological progression of Purkinje cell degeneration can be constructed at one time point postischemia to illustrate the nonapoptotic features of this cell death. (A) Normal Purkinje cells (arrows) in control cat; (B) during stage 1, the Purkinje cell body severely shrinks (arrows) and the nucleus becomes dark and shrunken. The Nissl substance is redistributed to the periphery of the soma (as contrasted with the perinuclear distribution of Nissl substance within the perikaryon in normal Purkinje cells, see A). The Purkinje cell dendrites become more prominent, signifying dendritic retraction and swelling of peridendritic astrocytic processes; (C) during stage 2, the cytoplasm of Purkinje cells (arrows) becomes homogenous as the Nissl staining is lost (the corresponding ultrastructural observation is fragmentation and loss of the rough endoplasmic reticulum, see Figs. 10, 11); (D) during stage 3, the Purkinje cell perikaryon (arrow) shows complete homogenizing cell change as the cytoplasm becomes uniform (i.e., eosinophilic or pink in hematoxylin and eosin preparations). At this stage, attack of inflammatory cells occurs. (E) At stage 4, Purkinje cells undergo severe cytoplasmic vacuolation and then dissolution; (F–H) postischemic degeneration of Purkinje cells (arrows) at stage 1 (F), stage 3 (G), and stage 4 (H). Note that the nucleolus is present until end-stage degeneration, unlike the rapid disintegration of the nucleolus in apoptosis. Scale bars: A, 11.7 μm (same for B–E); F, 6 μm (same for G and H).

of insult and whether its occurrence is acute ($\leq$24 h) or delayed (3–7 days). Therefore, we conclude that acute and delayed ischemic neuronal death is structurally, and perhaps mechanistically, identical. This conclusion is consistent with the principle of the maturation phenomenon [69]. In all of our models of global cerebral ischemia, neurodegeneration in selectively vulnerable regions is morphologically indistinguishable from the neuronal death caused by excitotoxicity, and, specifically, it closely resembles the neuronal death caused by NMDAreceptor activation in adult brain (Figs. 4A–I, 6A–F, 7A–F, 10A–I, and 11A–I). The morphology of

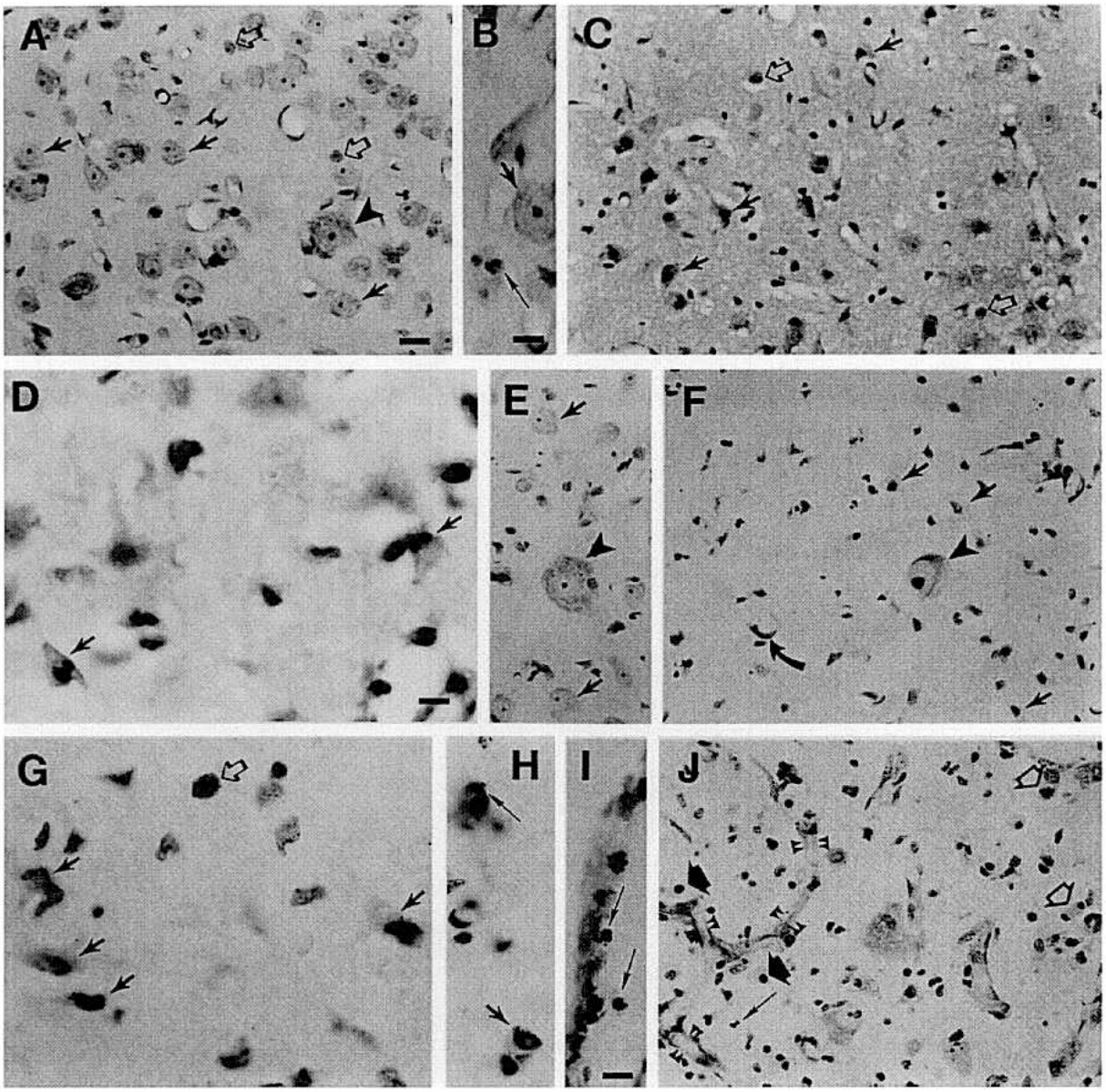

FIG. 9. Striatal degeneration in hypoxic-ischemic piglets. (A) Hematoxylin and eosin-stained section of control piglet striatum showing numerous round, medium-sized (10–20 μm) neurons (solid, black arrows) and less frequent large (20–40 μm) neurons (black arrowhead). Astrocytes with sparse cytoplasm can also be discerned (open arrows); (B) occasional apoptotic cells undergoing physiological cell death are encountered (thin black on white arrow) among normal medium-sized striatal neurons (black arrow) in control piglets; (C) many principal striatal neurons (black arrows) and subsets of large neurons (black arrowhead) show severe ischemic cell injury at 24 h recovery, as evidenced by the eosinophilic (pink) cytoplasm, nuclear pyknosis, and shrinkage of the cell body. By light microscopy, the vast majority of striatal neuron degeneration is not apoptotic. Astrocytes are swollen (open arrows), causing severe vacuolation of the neuropil and formation of perineuronal spaces; (D) at 24 h postischemia, a small subset of ischemic neurons (arrows) exhibit condensation of the nucleus into large, round clumps (compare with apoptotic cell in panel B); (E) in TUNEL/cresyl violet (CV) preparations of control putamen, principal neurons (black arrows) and magnocellular neurons (arrowhead) are not TUNEL-positive. Only rare, small TUNEL-positive cells are encountered in controls (not shown); (F) TUNEL/CV sections of piglet striatum at 24 h after hypoxia–ischemia show numerous medium-sized neurons (black arrows) and large neurons (arrowhead) are that TUNEL-positive. Capillary endothelial cells are also TUNEL-positive (curved arrow); (G) TUNEL/CV sections of hypoxic-ischemic piglet striatum at 24 h recovery show that TUNEL-positive medium-sized neurons (black arrows) are angular and shrunken, typical of ischemic neurons (faint labeling of the cytoplasm probably indicates leakage of fragmented DNA into the perikaryon, because the nuclear envelope is not intact, see Fig. 11). In contrast, TUNEL-positive astrocytes (open arrow) have a round/ellipsoidal nucleus without visible cytoplasm due to the swelling (compare with astrocytes in panels C and D). Nearby astrocytes (blue-stained cells in upper right) are not TUNEL-positive; (H) in the hypoxic-ischemic piglet striatum at 24 h, an unidentified TUNEL-positive cell (thin black on white arrow) with spherical clumps in the nucleus reminiscent of apoptosis (compare with panels B and D) can be distinguished from a TUNEL-positive neuron (black arrow) with less chromatin clumping and a prominent nucleolus; (I) by 48 h after hypoxia–ischemia, many small cells that have infiltrated into perivascular locations in the striatum are TUNEL-positive and undergo unequivocal apoptosis (thin black on white arrows). Their size and location indicate that they are dying leukocytes; (J) by 96 h after hypoxia–ischemia, the putamen shows elimination of neurons (compare with panel A) and gliomesodermal scarring. TUNEL-positive small, round cells with spherical nuclei are present (broad arrows), typically in the vicinity of microvessels (double arrowheads), and most likely represent apoptosis of macrophages. TUNEL-negative cells with characteristic apoptotic nuclei (thin black on white arrow) are sometimes encountered. Mitotic figures are also present (open broad arrows). Scale bars: A, 20 μm (same for C–F and J); B, 10 μm; G, 10 μm; I, 10 μm. Reproduced from [120] with permission from the American Neurological Association.

ischemic neuronal death and excitotoxic neuronal death induced by non-NMDA receptor activation is similar with respect to the cytoplasmic abnormalities but not the nuclear changes.

The progression of ischemic neuronal death is shown in principal striatal neurons of hypoxic–ischemic piglets (Figs. 10A–I and 11A–I). In this model, degeneration of principal striatal neurons occurs by 24 h [119,120]. This degeneration evolves in association with acute oxidative stress in the form of peroxynitrite-mediated nitration of proteins at 3–12 h after ischemia, possibly resulting from transient bursts in mitochondrial function [119]. Ultrastructural changes in the cytoplasm are detected before changes in the nucleus are demonstrable. By 3 h, neurons form many, clear, round membrane-bound vacuoles, the origin of which is still uncertain, but Golgi vesiculation is one possible source. In addition, the rough endoplasmic reticulum dilates, releases its ribosomes, and then becomes fragmented. Polyribosomes also disaggregate to form monosomes. Most mitochondria remain intact until approximately 6–12 h after ischemia, and then they swell and vacuolate and undergo cristaeolysis. From 6–12 h, the neurons darken and assume an angular shape, and the nucleus becomes pyknotic and forms irregularly-shaped clumps of chromatin that are distributed throughout the nucleus with a darkened matrix. During this process, the nucleolus remains obvious, unlike the early disintegration of the nucleolus in apoptosis. These degenerating neuronal profiles are usually surrounded by large, swollen astrocytic processes. Eventually, both cytoplasm and nucleus are digested and disintegrate within 12–24 h. This neuronal death following ischemia is very different from neuronal apoptosis (Figs. 1A–H, 2A, 3A–L, 10A–I, and 11A–I). It is important to emphasize that this temporal pattern of structural changes in neurons following cerebral ischemia is very similar to the subcellular evolution of cell death when plasma membrane function and ATP synthesis are impaired and is consistent with abnormalities in cell volume homeostasis [91,92, 130].

Location of Apoptosis After Global Ischemia

We detected apoptotic cell death in some neuronal groups that are not typically regarded as selectively vulnerable to ischemia (Fig. 12A–D). For example, subsets of granule cells in the dentate gyrus, subsets of granule cells in the cerebellar cortex, and certain neurons in thalamic nuclear groups appear apoptotic. In addition, prominent apoptotic death of white matter oligodendrocytes occurs, notably in hypoxic–ischemic newborn brain (Fig. 12A–D). The presence of apoptotic death in these groups of cells after global ischemia is possibly related secondarily to target deprivation or to axonal degeneration in response to ischemic degeneration of selectively vulnerable populations of neurons (see later).

In all of our models, perivascular and parenchymal nonneuronal cells undergo apoptosis (Fig. 9H–J). These nonneuronal cells are most likely hematogenously derived inflammatory cells, such as leukocytes and macrophages, which infiltrate into areas of neuronal damage. This inflammatory response, which occurs invariably in ischemia–reperfusion tissue injury [51,125], is a complicating variable in the interpretation of data obtained using nonhistological approaches, because of the inability to assign the contribution of specific cell types to the observation. Moreover, observations showing postischemic neuroprotection with protein synthesis inhibition may be influenced by alterations in the immune/inflammatory response process rather than a specific molecular interruption of a PCD mechanism within vulnerable neurons. For example, protein synthesis inhibitors influence T cell survival [9]. It is even possible to envision that changes in the normal immune system and inflammatory response modifies the evolution of ischemia-reperfusion injury in transgenic mouse models that overexpress (or do not express) genes for regulatory proteins that control cell death.

DNA Fragmentation Following Cerebral Ischemia

Brain damage following ischemia has also been analyzed with respect to breakdown of genomic DNA. By *in situ* DNA end labeling methods, many studies have shown that selectively vulnerable populations of neurons undergo nuclear DNA fragmentation following cerebral ischemia [12,65,66,112,128,140]. The expectation that neurons die following cerebral ischemia has been fulfilled by these reports. Nonneuronal cells (e.g., astrocytes, oligodendrocytes, inflammatory cells, vascular cells) also die following ischemia-reperfusion, and some of these nonneuronal cells appear apoptotic (Fig. 9F–J) [120]. By gel electrophoresis, DNA fragmentation patterns are regionally and temporally dependent following cerebral ischemia. In DNA extracted from brain regions of adult rat or gerbil, internucleosomal fragmentation has been found following transient global forebrain ischemia [14,65,112, 140,144] and focal ischemia [104,178]. The DNA digestion is thought to occur as a relatively late event in the course of ischemic cell death [178], and it has been suspected that cells undergoing internucleosomal DNA fragmentation coexist with cells undergoing random DNA digestion following ischemia [178]. Internucleosomal DNA cleavage has also been detected in hypoxic–ischemic immature rat brain regions [12,66]. However, in hypoxic–ischemic newborn piglet striatum, we detect a random pattern of DNA digestion with a temporal progression that is very consistent with acute oxidative damage and the morphological pattern of neuronal necrosis [119]. Despite these many reports of internucleosomal DNA breakdown in cerebral ischemia, solid morphological evidence for prominent apoptotic death of selectively vulnerable populations of neurons is still missing. The uncertainty about the contribution of apoptosis in ischemic neurodegeneration is exposed further when considering data showing that the morphological changes and the internucleosomal DNA fragmentation of apoptosis are inhibited by Zn^{2+} [35,189], yet neurons that die acutely or in a delayed fashion following global ischemia accumulate Zn^{2+} prior to degeneration [87].

Molecular Regulation of Programmed Cell Death Following Cerebral Ischemia

The identification of a variety of gene products that regulate programmed death of mammalian cells has provided another opportunity to explore the contribution of apoptosis to ischemic neurodegeneration. The *bcl-2* protooncogene and the caspase cysteine protease families are the best characterized to date. Bcl-2 and Bcl-x_L gene products can block apoptosis and promote cell survival, whereas *bcl-2*-related gene products, Bax and Bcl-x_S, are inhibitors of Bcl-2 function and promote cell death [131]. In mice that overexpress Bcl-2, infarct volumes caused by middle cerebral artery occlusion are ~40% smaller than those in wild-type littermate controls (in some coronal brain levels through the infarct territory) [123], but it is important to note that *bcl-2* transgenic mice have ~30% more neurons than nontransgenic mice in some brain regions [40]. However, overexpression of Bcl-2 in brain by infection with *Herpes simplex* virus vector containing the *bcl-2* gene does not affect infarct volume [96,103]. Following global ischemia in rat, Northern blot analysis shows increased expression of Bcl-2 and Bcl-x_L messenger RNA (mRNA) in neocortex and hippocampus at 24 h postischemia, and, by *in situ* hybridization analysis, expression of Bcl-2 and Bcl-x_L mRNA increases in CA1 and CA3 pyramidal layers and in the dentate gyrus granule cell layer at approximately 4–48 h postischemia [20]. However, at 72 h postischemia, Bcl-2 and Bcl-x_L mRNA levels in CA1 are reduced, corresponding to the degeneration of pyramidal neurons

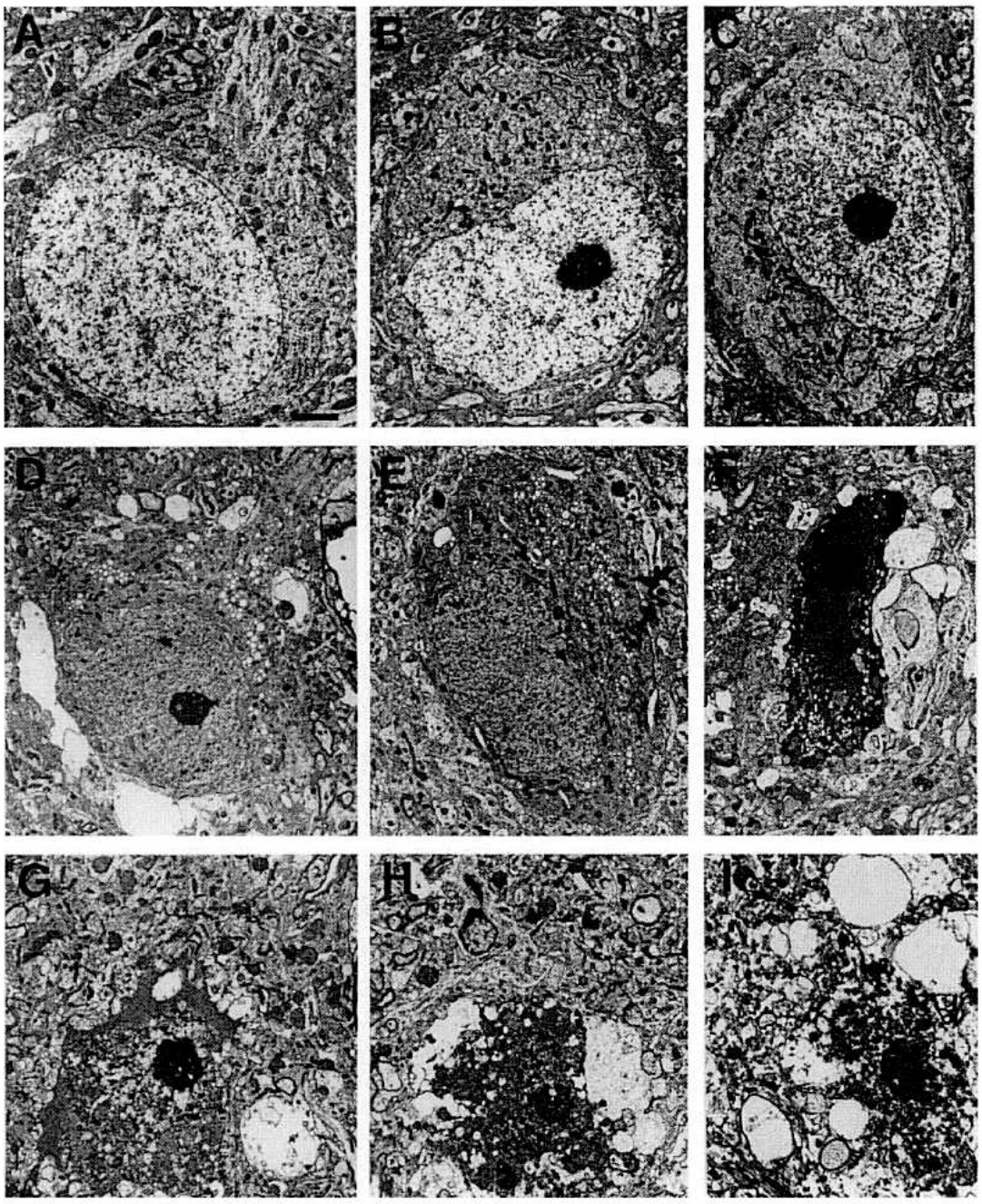

FIG. 10. Ultrastructural progression of principal neuron death in hypoxic-ischemic piglet striatum. A normal principal striatal neuron from a control piglet (A) is shown for comparison with neurons from piglets at 3, 6, 12, and 24 h after hypoxia-ischemia (B–I) arranged in a temporal sequence to show the predominant structural changes in ischemic neuronal necrosis. This neuronal death is not precisely synchronized because at any time point postischemia dying neurons can be found at different stages of degeneration. By 3 h after ischemia (B), many, clear vacuoles are formed within the cytoplasm, increasing progressively during the subsequent 3–6 h (C–E). During the 6-h period after ischemia (B–E), the arrays of rough endoplasmic reticulum become fragmented and the mitochondria become dark and condensed, as the cytoplasmic matrix becomes progressively dark and homogeneously granular. The overall contour of the cell changes from a round shape (A and B) to a fusiform and angular shape (C–E); as the neurons become shrunken (F). Concurrently, the nuclear matrix progressively becomes uniformly dark (C–E) and the nucleus becomes shrunken as numerous small, irregular clumps of chromatin are formed throughout the condensing nucleus (F). The nucleolus still remains prominent throughout this process (B–D, F), even until ultimate neuronal disintegration (G–I). From 12–24 h, injured cells disintegrate as the dark, severely, vacuolated cytoplasm, containing few discernible but very swollen mitochondria, undergoes dissolution, while the nucleus progressively forms more chromatin clumps and undergoes karyolysis (G–I). The cytoplasmic and nuclear debris is liberated into the surrounding neuropil (I). This neurodegeneration is morphologically necrotic, and is indistinguishable from ischemic degeneration of CA1 neurons and NMDA receptor-mediated excitotoxic death of striatal neurons (see Figs. 4, 7). Scale bar: A, 1.3 μm (same for B–I).

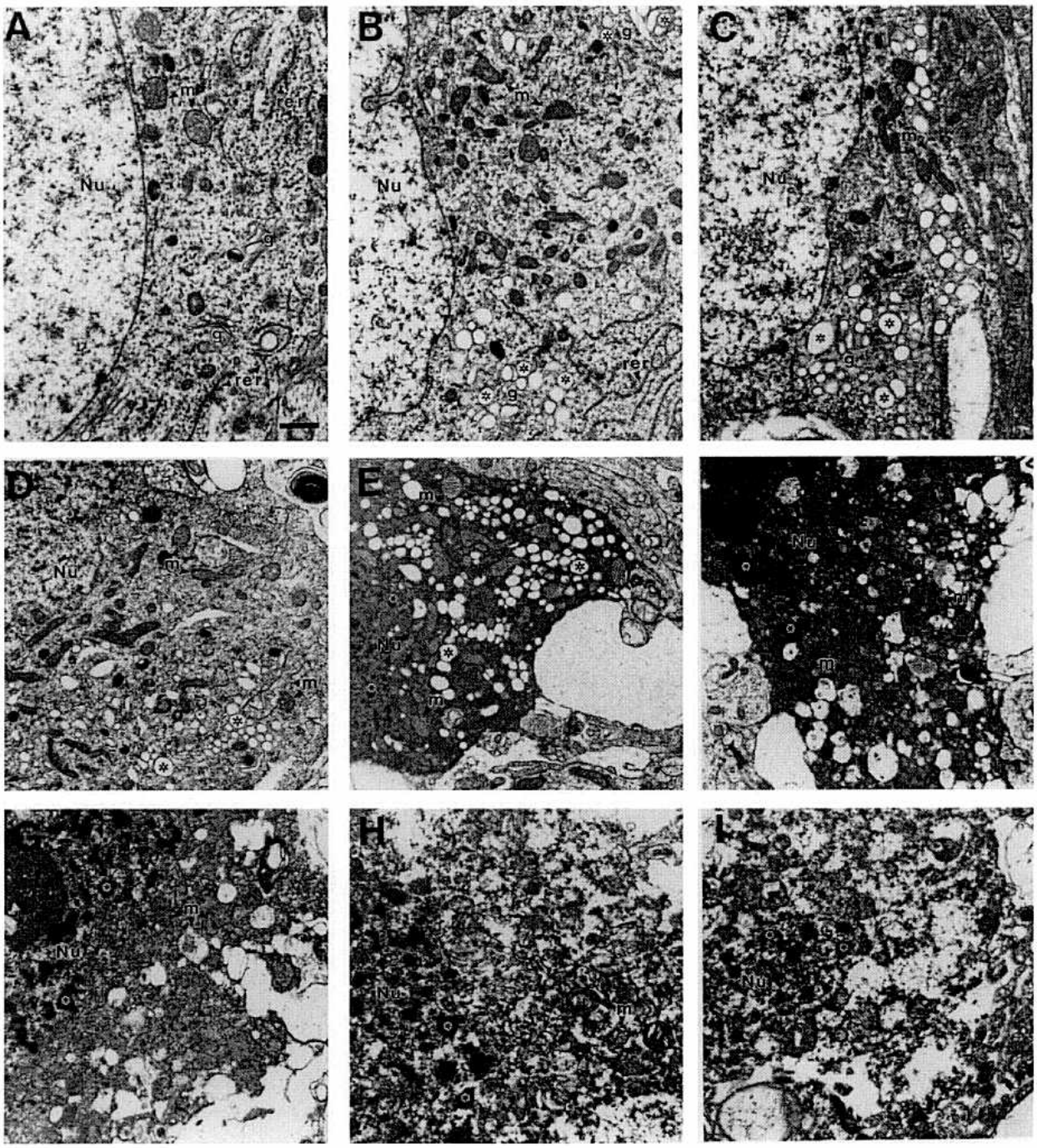

FIG. 11. The degeneration of striatal neurons in piglets following hypoxia–ischemia is associated with sequential and progressive subcellular abnormalities within the cytoplasm and then the nucleus that are consistent with cellular necrosis. Abbreviations: g, Golgi apparatus; m, mitochondria; Nu, nucleus; rer, rough endoplasmic reticulum. (A) In control piglets, normal, principal, striatal neurons have abundant polyribosomes distributed throughout the cytoplasmic matrix, intact arrays of rough endoplasmic reticulum and Golgi stacks, and uniformly shaped mitochondria with intact cristae; (B) by 3 h after ischemia, the Golgi complex swells and undergoes vesiculation to form clear vacuoles (asterisks). The mitochondria become condensed and distorted. The rough endoplasmic reticulum appears relatively normal, but some ribosomes are unbound from the rough endoplasmic reticulum and polyribosomes disaggregate with dispersal of free ribosomes in the cytoplasm causing the matrix to become granular; (C–E) by 6 h after ischemia, many Golgi-derived vacuoles accumulate (asterisks) as the surrounding cytoplasmic matrix becomes progressively granular and dark. The rough endoplasmic reticulum becomes disorganized and fragmented. Some mitochondria appear condensed but others are very swollen and exhibit cristaeolysis. The nucleoplasmic matrix progressively becomes darker and the chromatin undergoes condensation into small clumps of various sizes (asterisks, D, E), while the nuclear envelope becomes less discernible; (F) by 12 h after ischemia, the cytoplasmic matrix becomes homogeneously dark and most organelles are no longer discernible, except for swollen and degenerating mitochondria. Numerous, vacuoles containing membranous debris are formed in the cytoplasm as more mitochondria degenerate and undergo cristaeolysis. The nuclear chromatin becomes prominently aggregated into ill-defined clumps of various shapes and sizes, as the surrounding nucleoplasmic matrix becomes uniformly dark and the nuclear envelope looses integrity; (G–H) By 12–24 h after ischemia, the dark and condensed cytoplasm, containing degenerated mitochondria, undergoes fragmentation as the plasma membrane ruptures. The nucleus, containing chromatin clumps (asterisk), is no longer surrounded by an intact nuclear membrane and undergoes karyolysis; (I) at end-stage neuronal dissolution caused by ischemia, cytoplasmic debris and nuclear debris with chromatin clumps (asterisk) are dispersed into the surrounding neuropil. Scale bar: A, 0.5 μm (same for B–I).

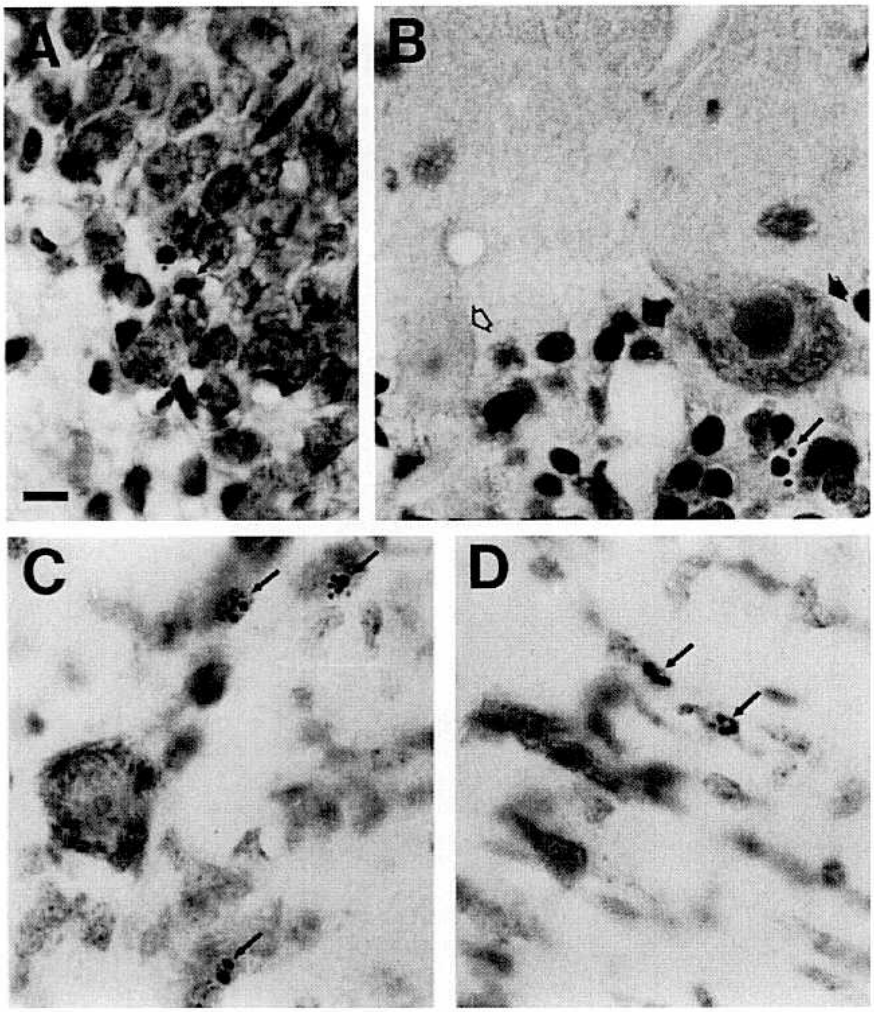

FIG. 12. Light microscopic evidence for apoptosis following transient cerebral ischemia. (A) Apoptosis of granule cells (arrows) in the hippocampal dentate gyrus at 7 days following incomplete global ischemia in dog; (B) apoptosis of cerebellar granule cells (arrow) in cat at 3 days following global ischemia. In the same microscopic field, necrotic Purkinje cell degeneration is at early stage 1 (solid black arrowhead) or stage 4 (open arrowhead); (C) apoptosis of cells (arrows) in reticular thalamic nucleus in piglet at 2 days recovery following hypoxia–ischemia; (D) apoptosis of oligodendrocytes in subcortical white matter (arrows) in piglets at 2 days following hypoxia–ischemia. Scale bar: A, 6 μm (same for B–D).

[20]. Bax mRNA is also increased after ischemia in both vulnerable and less vulnerable regions [21]. These analyses of mRNA following cerebral ischemia are difficult to interpret when considering the dramatic subcellular changes in organelles that function in protein synthesis and posttranslational processing (Figs. 10A–I and 11A–I), thereby potentially rendering the translation and formation of mature products inefficient. By immunoblotting, Bcl-2 and Bcl-x_L protein levels appear to be increased in hippocampus as well, but immunocytochemistry shows that nonneuronal cells may account for this apparent increase [20]. Changes in Bax protein levels, as determined by immunoblotting, are conflicting in rat hippocampus following global ischemia. For example, one study demonstrated a transient increase at 6 h postischemia and then subsequently no change relative to control [88], whereas another study demonstrated a sustained increase in Bax protein levels [21]. Interestingly, although mRNA and protein levels for the proapoptotic cysteine protease ICE (interleukin-1β-converting enzyme/caspase-1) are increased in hippocampus following global ischemia in gerbils, this change is associated with inflammatory cells rather than selectively vulnerable CA1 pyramidal neurons [14].

Ischemic Neurodegeneration: Conclusions and Future Directions

The discrepancies between the morphological features of necrosis and the DNA fragmentation signature of apoptosis during ischemic neurodegeneration may have several explanations. Internucleosomal DNA fragmentation can occur in *in vitro* models of Ca^{2+}-induced cell death with ultrastructural features of necrosis [26] and in neuronal necrosis induced by NMDA receptor-mediated excitotoxicity [59,152]. These observations are not surprising in light of the role of Ca^{2+} in the activation of some endonucleases

responsible for DNA cleavage [8]. In this regard, it is noteworthy that Ca^{2+}-treated hepatocyte nuclei show internucleosomal DNA fragmentation while exhibiting a nuclear morphology consistent with cellular necrosis [143]. Furthermore, the ultrastructure of Ca^{2+}-treated hepatocyte nuclei is very similar to the nuclear morphology in necrotic neurons following ischemia and NMDA receptor excitotoxicity [152]. These findings raise questions regarding the usefulness of using internucleosomal DNA fragmentation as the sole criterion for identifying apoptosis [26]. Indeed, changes in genomic DNA integrity and cell morphology during death may vary independently of one another [26,59,152]. In apoptosis, internucleosomal DNA fragmentation in thymocytes takes place early in the process of cell death and may be a direct cause of cell death [8], although this conclusion has been disputed by others using hepatocyte cultures [143]. In ischemic neuronal death, morphological evidence for cell injury appears to precede internucleosomal DNA fragmentation [119,178]. Perhaps in ischemic and excitotoxic neuronal death, internucleosomal DNA fragmentation should be viewed as a transient, temporal stage of ongoing DNA digestion during cellular necrosis (that depends on different degrees of protease coactivation), but not as a marker for apoptotic cell death. However, the detection of internucleosomal DNA fragmentation *in vivo* may in fact reflect *bona fide* apoptosis, but of cells other than the selectively vulnerable neurons that are directly destroyed by a mechanism associated with cellular necrosis. Alternatively, neuronal death caused in ischemia, excitotoxicity, and PCD may share some overlapping biochemical and molecular mechanisms that result in neuronal degeneration that is a hybrid of classic apoptosis and classic necrosis. Therefore, the conventional way of classifying cell death into only two categories may not be appropriate for induced neuronal death, particularly when multiple morphological phenotypes for neuronal death have been identified [24,150–153].

An important, unresolved question regarding the pathobiology of ischemic neurodegeneration is whether the absence of the classic apoptotic morphological phenotype in selectively vulnerable populations of neurons is sufficient evidence to exclude the possibility that PCD may be operative. In answering this question, it is important to recognize that all forms of PCD may not occur via apoptosis [166]. For example, the death of T cells during negative selection in mouse thymus and the death of intersegmental muscles during metamorphosis in the moth *Manduca sexta* both occur by PCD; however, these cell populations die with distinct morphological and biochemical phenotypes [166]. Therefore, some cells can use a PCD mechanism that is not associated with the structure of apoptosis. Clearly, much more work is needed to answer this complex question as it may relate to ischemic neurodegeneration.

Despite the use of various techniques (e.g., electron microscopy, DNA fragmentation analysis, Northern analysis, reverse transcriptase polymerase chain reaction, *in situ* hybridization, immunoblotting, immunocytochemistry), studies still fail to provide irrefutable evidence that directly supports the hypothesis that postischemic degeneration of selectively vulnerable populations of neurons is apoptosis occurring by a PCD mechanism, rather than a process resulting in neuronal necrosis. Recent data on postischemic changes in cell death proteins of the Bcl-2 family are less meaningful out of the context of possible alterations in the interactions among these proteins, by which they function [131]. Future experiments using transgenic and gene-ablated mice may provide more data on whether apoptosis has a major, direct contribution in delayed neurodegeneration following ischemia. However, this expectation is contingent upon the development of mouse models of global cerebral ischemia with reproducible neuropathology.

NEURONAL DEATH IN TARGET DEPRIVATION AND AXOTOMY

Naturally-Occurring Cell Death During CNS Development

The occurrence of normal neuronal death in the developing nervous system is well established (Fig. 1A–H) [23,52,61,62,141, 150] and is thought to function in regulating the size of neuronal groups in relation to target size and synaptic inputs [25,102,147]. This developmental neuronal death (particularly of spinal and sympathetic ganglion neurons and motor neurons) is thought to be partially controlled by the supply of neurotrophic factors from the target [61,147]. However, an active role for some neurotrophins in the survival of developing motor neurons is uncertain [58], because gene ablations of brain-derived neurotrophic factor [37,74], ciliary neurotrophic factor (CNTF) [124], neurotrophin-3 [39], and neurotrophin-4 [107] have no effect on motor neuron survival during the PCD period (although sensory ganglionic neuron survival is usually influenced). Yet, CNTF-ablated mice show a progressive, age-related degeneration of motor neurons [124], an observation that encouraged the use of this molecule in clinical trials for the treatment of motor neuron degeneration in ALS [10].

Developmental neuronal death is regulated by cell death proteins, because mice that overexpress the *bcl-2* gene [40,123] or have *bax* gene-ablations [30] have increased numbers of neurons in some nervous system regions, whereas *bcl-2*-deficient mice show progressive neuronal degeneration after the PCD period [132]. Other data support a role for caspases in the survival of sensory and motor neurons. Inhibition of caspase-1 (ICE) and caspase-2 blocks the apoptosis of dorsal root and sympathetic ganglion neurons when deprived of nerve growth factor (NGF) [31,46]; furthermore, inhibition of caspase-1 arrests the PCD of motor neurons *in vitro* resulting from trophic factor deprivation and *in vivo* during the period of naturally occurring cell death [134].

PCD and Human Neurodegeneration

The concept of PCD and recent findings regarding the molecular regulation of PCD have kindled the idea that mutations or other abnormalities in cell death proteins, trophic factors, or their receptors, as well as target deprivation and retrograde neuronal injury may participate in the evolution of abnormal neuronal death in progressive neurodegenerative diseases [15,124,131,155]. This possibility is supported by the finding that the genes for neuronal apoptosis inhibitory protein and survival motor neuron protein are either deleted partially or are mutant in some children with spinal muscular atrophy [97,161] and by the finding that abnormalities in the balance of Bcl-2 and Bax may occur in spinal motor neurons in ALS [137]. In addition, subsets of neurons undergo nuclear DNA fragmentation in ALS [182,197] and in AD [4,111], although this DNA digestion is partly related to postmortem autolysis [4,111]. However, evidence for *in situ* DNA fragmentation in ALS and AD has not been found by others [133]. It is still uncertain whether the neurodegeneration in ALS and AD is related causally to target deprivation and abnormalities in trophic factors or cell death proteins and whether neuronal apoptosis contributes to this degeneration. Dying neurons with apoptotic morphologies have not been detected in these diseases [111,197,133]. In disorders like ALS and AD, rational and effective treatment is difficult to administer without a better understanding of the pathogenesis of neuronal death in the adult CNS.

Animal Models of Axotomy and Target Deprivation

To gain insight into the mechanisms of progressive neuronal injury and degeneration, animal models of axotomy and target

deprivation in different systems have been studied for many years [1,23,29,49,95,101,127,141,181]. Several factors influence the progression of axotomy-induced neuronal injury and the likelihood of subsequent neuronal death or survival, including whether the cell body of an axotomized neuron resides within the peripheral nervous system or CNS, the age of the animal at the time of injury, the location of axonal trauma in relation to the cell body, and the species [43,101,179]. In the immature nervous system, axotomized neurons often die rapidly, whereas, in the adult nervous system, axotomized neurons are more likely to recover or persist in some altered form [95,101,150,154,179]. For example, transection of the VIIth cranial nerve or sciatic nerve in newborn rodents causes loss of motor neurons in the facial nucleus or in the lumbar cord, respectively. In contrast, a similar lesion in adults produces no discernible loss of motor neurons [29,154]. In other models of axotomy and target deprivation, excitotoxic ablation of hippocampus in immature rat appears to cause death of septal cholinergic neurons [27], but in adult rat following fimbria-fornix transection (a complex model of target deprivation/axotomy and retrograde degeneration of medial septal neurons as well as partial glutamatergic deafferentation of lateral septal neurons [49]), axotomized septohippocampal projection neurons appear to atrophy and survive rather than die [49,60,138,148]. Interestingly, excitotoxicity appears to contribute to the injury and subsequent atrophy of populations of septal neurons in adult brain following fimbria-fornix transection [49,50].

Axotomy-induced degeneration of motor neurons in the immature CNS appears to be apoptosis, based on morphological evidence in mouse [160] and chick [23,141] and on the finding that *bcl-2* overexpression ameliorates the motor neuron death in newborn mice in response to facial nerve transection [34] or sciatic nerve transection [40]. However, *bcl-2* transgenic mice have more motor neurons than wild-type mice [40]. Although degeneration of axotomized motor neurons can be delayed by a variety of neurotrophic factors, these neurotrophins fail to prevent the ultimate death of target-deprived motor neurons over long term [36,187]. Glutamate receptors and excitotoxic mechanisms also participate in the death of axotomized motor neurons in newborns, because the susceptibility of spinal motor neurons to NMDA receptor toxicity is enhanced after nerve transection [57] and blockade of NMDA receptors [129] or non-NMDA glutamate receptors [70] rescues neonatal motor neurons that are destined to die after axotomy. A link between glutamate receptor activation and the induction of apoptosis in developing neurons has been revealed in studies demonstrating that excitotoxic lesions in the neonatal rat brain cause neuronal apoptosis (Fig. 3A–L) [152,153,186]. Other experiments demonstrate that NMDA receptor blockade prevents the normal death of mistargeted retinal ganglion cells [17]. Overall, these observations demonstrate that motor neuron survival in the immature CNS after injury is dictated by highly complex interactions between the target, neuronal excitability, and cell death programs, the details of which have yet to be clarified.

Axotomy and Target Deprivation of Geniculocortical Projection Neurons Causes Apoptosis in Adult Brain

Neurodegenerative diseases such as ALS and AD are adult-onset disorders. Therefore, the need arises for the use of animal models of target deprivation and axotomy to study the degeneration and death of neurons in the adult CNS. However, only a few models exist for studying axotomy-induced death of central neurons in adult animals. In one model, ablation of the occipital cortex in the adult mammalian brain reproducibly causes retrograde degeneration and apparent elimination of subsets of neurons in the lateral geniculate nucleus [11,93,94,127]. Because geniculocorti-

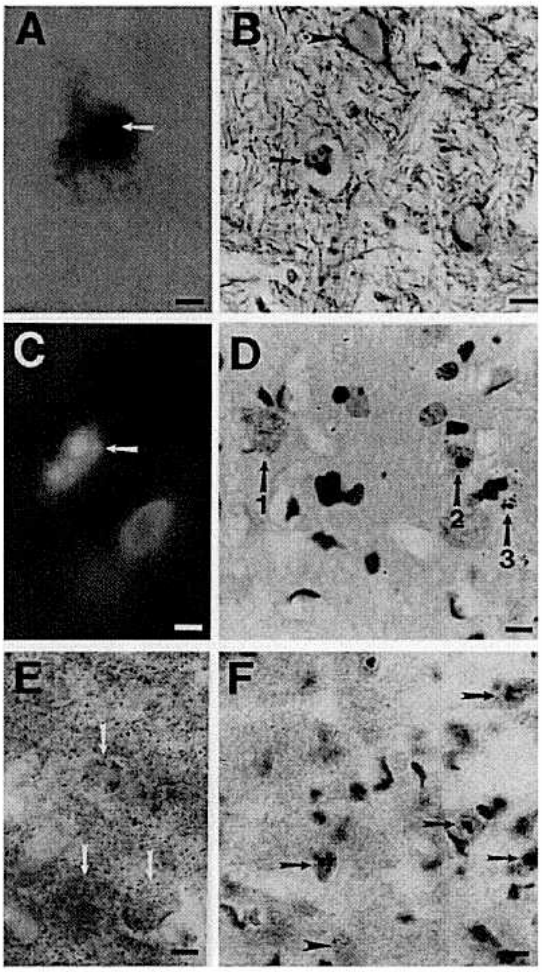

FIG. 13. Target deprivation causes apoptotic death of corticopetal neurons in the dorsal lateral geniculate nucleus (dLGN) following cortical ablation. (A) A TUNEL-positive, dLGN neuron (arrow) at 7 days following target deprivation; (B) immunostaining for neurofilament and cresyl violet counterstaining show that shrunken, degenerating cells with apoptotic chromatin clumps are neurons (arrow). Neurofilament immunoreactivity highlights the periphery of an apparently normal neuron (arrowhead); (C) retrograde prelabeling with Fluorogold (FG) shows that these dying neurons are geniculocortical projection neurons. By fluorescence microscopy, faint yellow cytoplasmic FG labeling is detected within degenerating neurons (arrow) and simultaneous staining with the nuclear dye DAPI (light-blue) reveals the chromatin clumps consistent with apoptosis; (D) immunocytochemical detection of FG labeling and Nissl counterstaining also shows that dying cells are geniculocortical projection neurons within the dLGN. The FG immunoreactivity (brown) is detected in apparently healthy corticopetal neurons (arrow 1) and in apoptotic corticopetal projection neurons (arrow 2) with a shrunken, irregular cell body and a dark, condensed nucleus, much like the preclumping nuclear condensation stage of apoptosis seen by electron microscopy (see Figs. 14 and 15). Note the brown granular FG immunoreactivity in the cytoplasm of both neurons. At a later stage of apoptotic neurodegeneration (arrow 3), the FG labeling is more difficult to appreciate, presumably because the cytoplasmic contents have been dispersed into the neuropil (see Figs. 14, 15); (E) high levels of mitochondrial cytochrome c oxidase activity (black reaction product) are detected in large cells (arrows) in the LGN following target deprivation; (F) oxidative damage to nuclear DNA occurs concurrently with apoptosis of retrogradely degenerating neurons (arrows) in the LGN following target deprivation. Immunocytochemical detection of hydroxydeoxyguanosine (a marker for oxidative damage to DNA) is found in the nucleus of neurons undergoing apoptotic chromatin condensation (arrows) but not in normal cells (arrowhead). Scale bars: A, 5 μm; B, 15 μm; C, 6 μm; D, 15 μm; E, 5 μm; F, 15 μm.

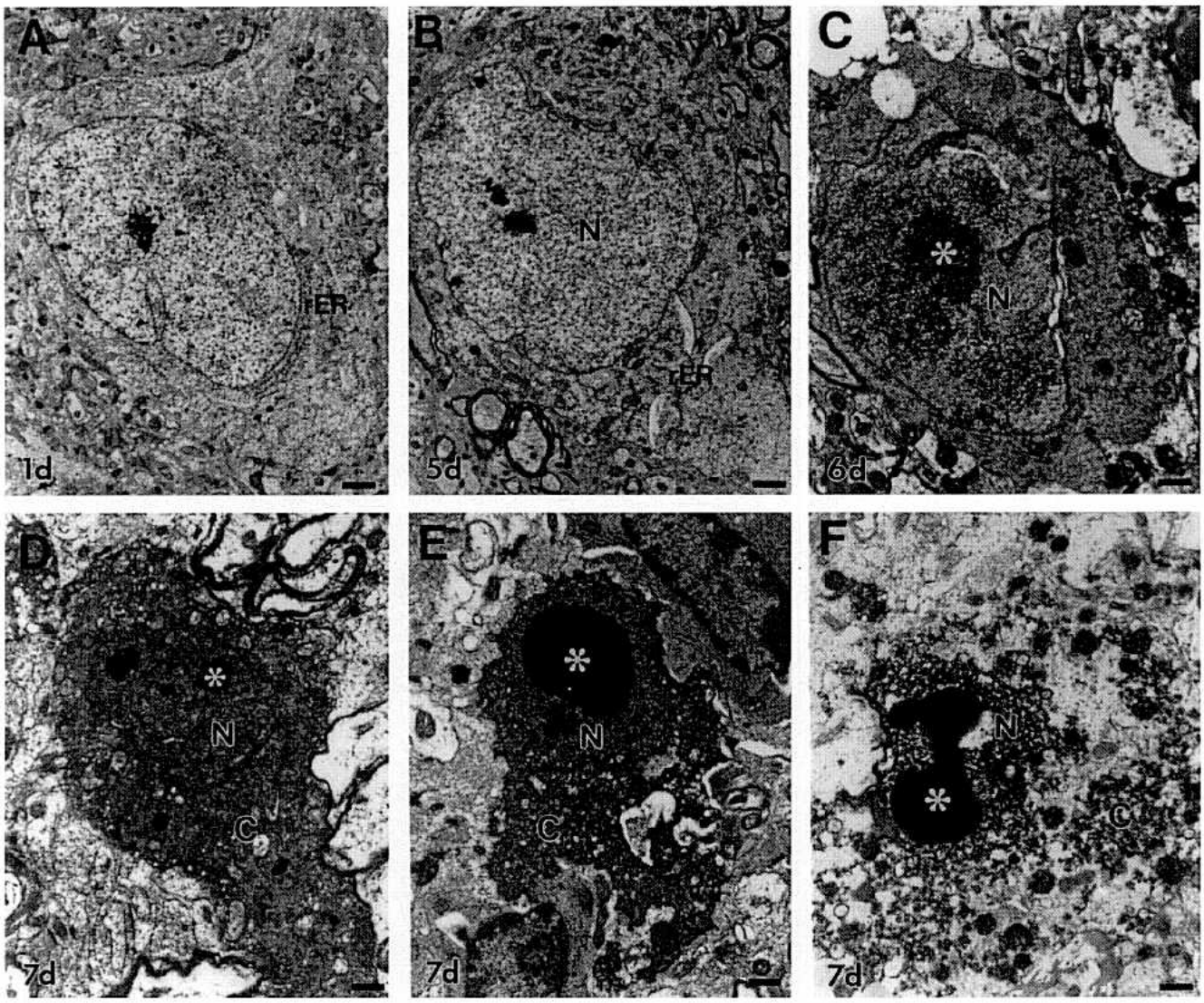

FIG. 14. Degeneration of target-deprived dLGN neurons ultrastructurally resembles apoptosis. Abbreviations: C, cytoplasm; N, nucleus; rER, rough endoplasmic reticulum. (A) At 1 day postlesion, neurons in the ipsilateral dLGN appear healthy, with normal perinuclear distribution of rough endoplasmic reticulum; (B) by 5 days, the rough endoplasmic reticulum fragments into truncated, randomly-oriented, curved arrays, while free ribosomes are dispersed. Golgi cisterns are swollen. Mitochondria, which remain intact, appear more numerous. The nucleus still appears essentially normal (but with a slightly darker and granular matrix); (C) by 6 days, the cytoplasm becomes darker and homogenous and is organized into compact laminations. While the rough endoplasmic reticulum and Golgi apparatus are indistinct, mitochondria are recognizable but some are swollen and degenerating, forming large vacuoles. At this time the nucleus becomes prominently darker and begins to show chromatin aggregation (asterisk); (D–F) At 7 days postlesion, dying neurons are at degenerative stages ranging from mid-apoptosis (D) to late apoptosis (F); (D) at midapoptotic stages, neurons become dark and shrunken. The condensed cytoplasm (C) contains numerous small and large vacuoles, with the larger vacuoles derived from degenerating mitochondria. The nucleus (N) begins to form round, compact chromatin clumps embedded within a homogeneously condensed nuclear matrix; (E) dying neurons then undergo extensive shrinkage and distortion of their perikaryon. The condensed cytoplasm (c) becomes perforated and vacuolated. The nucleus (N) forms large, round chromatin clumps (asterisk), representing the inner compact nuclear compartment, within a homogeneously dense nucleoplasm, representing the peripheral dense matrix, that is still surrounded by a nuclear membrane. The cell plasma membrane then disintegrates and the aggregated cytoplasmic contents are liberated into the surrounding neuropil with nearby oligodendrocytes. The peripherally condensed nuclear matrix (N), surrounded by a partially intact nuclear membrane, then becomes reticulated, while the large, round chromatin clumps (asterisk) appear stable; (F) when dispersal of cytoplasmic debris (c) is advanced, the nuclear envelope subsequently ruptures and the peripheral dense nuclear matrix (N), surrounding the compact chromatin clumps (asterisks), is then liberated into the neuropil. Scale bars: A, 2 μm; B, D, 1.75 μm; C, E, F, 1.5 μm.

cal projection neurons target highly focal regions of visual cortex with minimal collateralization [93,94], we hypothesized that target deprivation in this system would cause rapid and synchronized death of neurons in the dorsal lateral geniculate nucleus (dLGN) in adults, similar to the responses described for adult retinal ganglion cells after axotomy [13,158].

We found that occipital cortex ablation in the adult rat causes death of thalamocortical projection neurons in the dLGN (Fig.

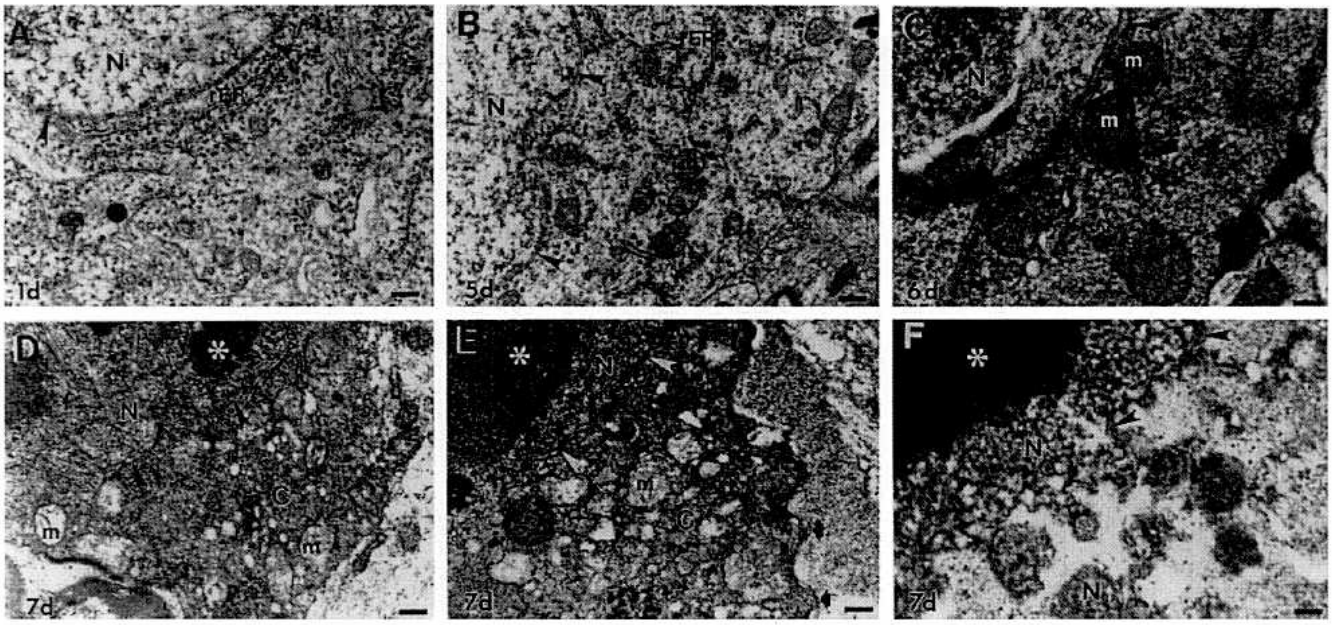

FIG. 15. Subcellular changes in degenerating adult dLGN neurons following target deprivation are consistent with apoptosis. (A) At 1 day postlesion, dLGN neurons appear healthy with normal rough endoplasmic reticulum (rER), Golgi apparatus, and mitochondria (m). The nucleus (N) and nuclear envelope (arrowheads) also appear normal; (B) by 5 days postlesion, the rER is conspicuously fragmented and free ribosomes, appearing as granules, are dispersed throughout the cytoplasm. Intact mitochondria (m) accumulate in the perikaryon. The nucleus (N) and nuclear envelope (arrowheads) appear normal; (C) by 6 days postlesion, dying neurons enter a stage of condensation. The cytoplasm becomes homogeneously granular and dark with a few small vacuoles. While rER and Golgi apparatus are indiscernible, most mitochondria (m) appear intact but are embedded in a dense cytoplasmic matrix. The nucleus (N) shows incipient chromatin condensation, becoming dark and aggregated, while the double-membrane nuclear envelope remains intact (arrowheads); (D–F) at 7 days postlesion, degenerating neurons progressively undergo a rapid sequence of cytoplasmic and nuclear changes leading to advanced condensation and then cellular dissolution (illustrated sequentially as D, E, and F). (D) The cytoplasm (C) of dying neurons becomes fused and electron opaque, containing many small vacuoles. Most mitochondria (m) are degenerating and appear as larger vacuoles containing remnants of the inner membrane. The nucleus (N), surrounded by a less conspicuous nuclear envelope (arrowheads), appears condensed and dark and begins to form small, compact chromatin clumps (asterisk); (E) the condensed cytoplasm (C) then forms larger vacuoles, some of which are degenerated mitochondria (m), while the cell plasma membrane becomes ruffled (arrows). The nucleus then undergoes a process of binary chromatin condensation into large, dark, round clumps (asterisk), representing the inner compact compartment, surrounded by a less-compact, homogeneously condensed nucleoplasm representing the peripheral dense nuclear matrix (N). At this time, the nuclear envelope appears undulated (arrowheads); (F) in the final stage, the plasma membrane disintegrates and the fused cytoplasmic contents are dispersed into the surrounding neuropil. Soon thereafter, the nuclear envelope ruptures (arrowheads), and fragments from the peripheral dense nuclear matrix (N) bud into the disintegrating cytoplasm and surrounding neuropil, while the inner compact nuclear compartment (asterisk) becomes progressively more exposed to the surrounding neuropil. Scale bars: A, 0.6 μm; B, 0.5 μm; C–F, 0.4 μm.

13A–F) and that this retrograde neurodegeneration has a phenotype that closely resembles apoptosis (Figs. 14A–F and 15A–F) [1]. This retrograde neurodegeneration of dLGN neurons evolves morphologically, over 7 days, from classical chromatolysis to apoptosis (Figs. 14A–F and 15A–F). Using ultrastructural criteria, we developed a novel staging scheme for classifying the progression of apoptotic, retrograde neurodegeneration [1]. These sequential stages are prechromatolytic (days 1–2), chromatolytic (days 3–5), early apoptotic (day 6), and late apoptotic (day 7). Chromatolysis in these neurons is followed by fragmentation of the rough endoplasmic reticulum, as well as dilatation and vesiculation of the Golgi complex, and accumulation of active mitochondria [1,2]. The chromatolytic response, including redistribution and dispersion of the rough endoplasmic reticulum with an increase in free ribosomes, occurs at approximately 3–5 days postlesion. Chromatolysis has been thoroughly characterized following axotomy and is associated with increased protein synthesis [101]. Chromatolysis following axotomy can be blocked or delayed when RNA synthesis is inhibited with actinomycin D [180], thereby implicating activation of gene transcription and protein synthesis as participatory in this neuronal response to injury. This finding is noteworthy in the context that PCD, a mechanism for apoptosis, can be prevented by inhibitors of RNA and protein synthesis [48,78,168].

Neurodegeneration in Axotomy/Target Deprivation: Conclusions and Future Directions

We conclude that if neurons, which have undergone axotomy and deprivation, fail to reestablish connections with their major sustaining targets, these chromatolytic neurons enter into a cell death pathway and then progress rapidly through end-stage apoptosis (Figs. 14A–F and 15A–F) [1]. The transition between chromatolysis and early apoptosis coincides with accumulation of structurally intact and functionally active mitochondria within the perikaryon at about 5 days postlesion [2]. This accumulation of mitochondria in axotomized dLGN neurons has been suggested by others as well [11,127,191]. The accumulation of mitochondria within the perikaryon may result from abnormal trafficking of mitochondria into axons and dendrites, because of damage to these compartments or because of neurocytoskeletal abnormalities [1]. This new *in vivo* finding [2] is important because mitochondria are thought to participate in the effector stage of apoptosis [89,198] by providing a rich source of ROS or by changes in Bcl-2 (located in

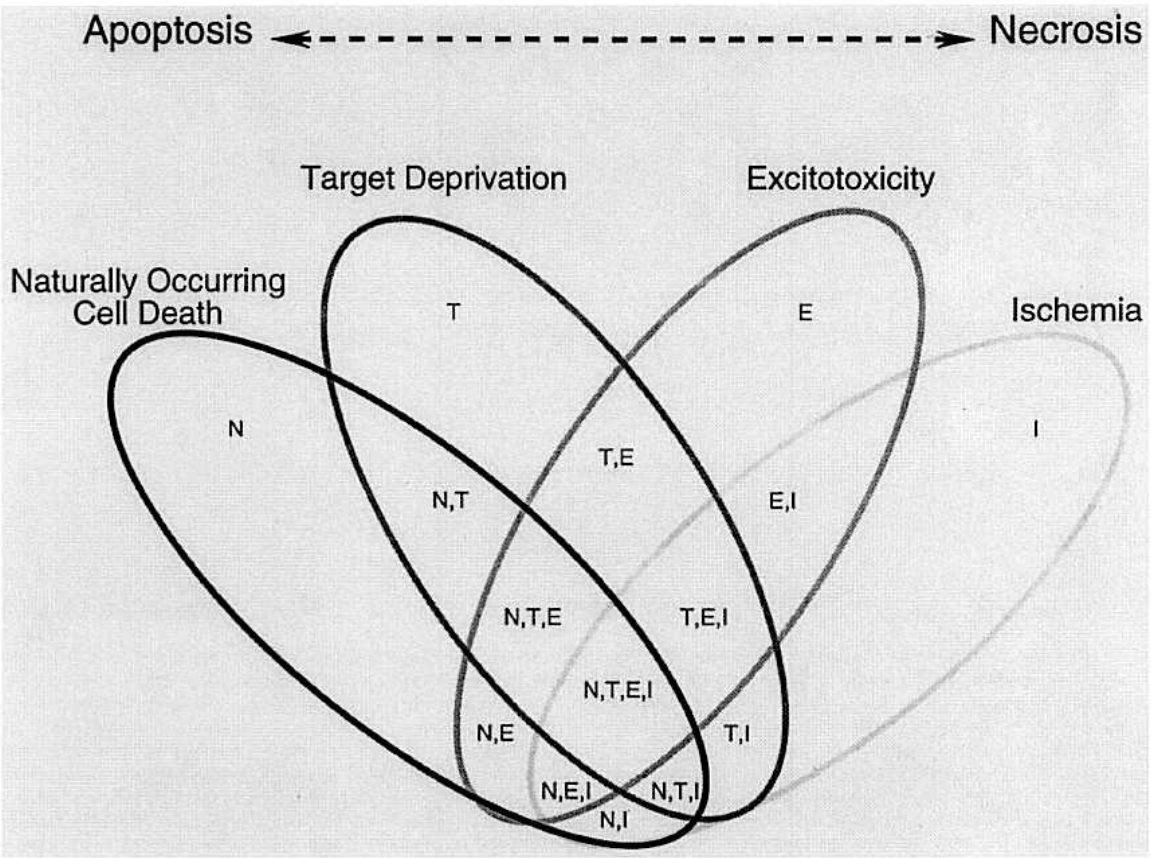

FIG. 16. Schematic diagram illustrating the potential relationships among naturally occurring cell death (N) and induced cell death in response to target deprivation (T), excitotoxicity (E), and ischemia (I) in the CNS as well as their relative positions along the apoptosis–necrosis continuum. Each ellipse represents a different setting of cell death. Naturally occurring cell deaths and target deprivation-induced cell deaths closely resemble apoptosis. Excitotoxic neuronal death in the developing brain can resemble apoptosis and necrosis, but in adult brain it resembles necrosis (NMDA receptor toxicity) and a hybrid of apoptosis-necrosis (non-NMDA receptor toxicity). Ischemia-induced cell death in selectively vulnerable neurons resembles necrosis and is structurally identical to NMDA receptor toxicity. Each setting for cell death has mechanistic components that may be distinct from the other settings (as indicated by the lack of overlap); however, some of the underlying mechanisms (most of which are not precisely identified) in each of these settings of naturally occurring and induced cell deaths may be shared to varying degrees (as indicated by the overlapping areas) and differ by rate of injury (e.g., evolution of oxidative stress). For example, oxidative stress in target deprivation/axotomy evolves slowly and the neuronal death has an apoptotic phenotype, but oxidative stress evolves acutely in ischemia and the neuronal death is necrotic. Target deprivation and glutamate receptors may have participatory roles in naturally occurring cell death as well as shared interactions among each other (see text for examples). In ischemia, where cell death is mostly necrotic, excitotoxicity has a prominent representation, but target deprivation-induced cell death may occur as well (in response to loss of selectively vulnerable neurons) and this may be a form of naturally occurring cell death which is apoptotic.

the outer mitochondrial membrane [106]), which has antiapoptotic functions that act through antioxidant pathways [67], or by blocking release of cytochrome c [86,196], which activates the caspase cascade [99,108,109]. We have also found that apoptotic dLGN neurons exhibit oxidative damage to nuclear DNA (Fig. 13F) [2]. The finding that oxidative stress induces neuronal apoptosis *in vitro* [89,159] supports our idea that mitochondria and oxidative damage participate in the transition of axotomized dLGN neurons from the chromatolytic stage to the early apoptotic stage. Most mitochondria in injured dLGN neurons at transitional and early apoptotic stages are normal ultrastructurally and appear to retain cytochrome c oxidase activity (Fig. 13E) [2]. If normal trafficking of these organelles into axonal and dendritic compartments is not reestablished, a sustained accumulation of mitochondria in the vicinity of the nucleus may provide a source of ROS that damage DNA. Once dying dLGN neurons reach the early apoptotic degenerative stage at approximately 6 days postlesion, the evolution through mid-apoptotic and late-apoptotic stages is rapid (requiring ~ 24 h or less for cellular elimination). This quick passage through the later stages of the apoptotic cell death process in dLGN neurons following cortical ablation is consistent with the rate of progression of apoptosis in chick embryo optic tectum [19] and in cell culture following neurotrophin deprivation [151].

Critical evaluation of the morphology of dying dLGN neurons reveals that this neurodegeneration is not completely identical to naturally occurring neuronal death during development (Fig. 1A–H) [153], to apoptotsis of nonneuronal cells in the dLGN following occipital cortex ablation [1], and to retinal ganglion cell death following optic nerve transection [13,158]. The death of adult dLGN neurons that we have described is unlike classic apoptosis because of differences in the progression and appearance of the nuclear changes, and the lack of detection of traditionally

TABLE 1

CONTRIBUTIONS OF APOPTOSIS AND NECROSIS TO VARIOUS FORMS OF NEURODEGENERATION

Model of Neurodegeneration	Cell Death Classification
Naturally occurring developmental cell death	Apoptotic, but some forms can fall along the apoptosis-necrosis continuum [24,153]
Axotomy/target deprivation	Apoptosis in the adult CNS (when neuronal death occurs) [1,2]
Excitotoxicity	Apoptotic, necrotic, and hybrid forms; falls along the apoptosis-necrosis continuum [152,153]
Global ischemia	Necrosis of selectively vulnerable neurons (CA1 and neocortical pyramidal neurons, Purkinje cells, and principal striatal neurons); apoptosis of inflammatory cells and oligodendrocytes; possible apoptosis of target-deprived neurons due to loss of selectively vulnerable neurons

described apoptotic bodies. Our conclusion that the death of geniculocortical neurons in the adult CNS closely approximates apoptosis is based on the general morphology and subcellular progression of this neuronal death that is induced by target deprivation. However, it possibly does not fully achieve classic apoptosis because of the principle that neuronal maturity may influence cell death morphology [150,152,153], such that immature neurons are more likely than mature neurons to die with a definite apoptotic morphology following injury. Alternatively, death of these adult dLGN neurons may be merely a variant of apoptosis, because many forms may exist in the CNS [24].

GENERAL CONCLUSIONS ON THE CONTRIBUTIONS OF APOPTOSIS AND NECROSIS TO NEURODEGENERATION

Neuronal degeneration in the CNS exists as a continuum between apoptosis and necrosis (Fig. 16). This morphological continuum is defined as the occurrence of classic apoptosis and necrosis at opposite ends of the spectrum of cell death, with many possible variant forms of cell death residing between the classic endpoints. Naturally occurring neuronal death in the developing CNS is phenotypically apoptosis (Fig. 1A–H, Table 1). Excitotoxin-induced neuronal death can appear as apoptosis, necrosis, and as hybrids of apoptosis and necrosis (Figs. 2A–C, 3A–L, 4A–I, 5A–I, and 6A–F, Table 1). Ischemia-induced degeneration of selectively vulnerable neurons is phenotypically necrotic (Figs. 7A–F, 8A–H, 9A–J, 10A–I, and 11A–I, Table 1), but apoptosis occurs in some neurons and in nonneuronal cells (Fig. 12A–D), possibly in response to degeneration of selectively vulnerable neurons. Target-deprivation induces neuronal death that closely resembles apoptosis (Figs. 13A–F, 14A–F, and 15A–F, Table 1) but is not identical to naturally occurring neuronal death in development. Therefore, the occurrence of neuronal apoptosis and necrosis in the injured CNS may not be obligatory, mutually exclusive forms of cell death. Some forms of induced neurodegeneration (notably those that occur with excitotoxicity) may be hybrids with coexisting mechanisms that dictate a wide range of apoptotic and necrotic phenotypes expressed by dying neurons. This range in neuronal death phenotype is likely to be influenced by many factors. For example, the mechanistic rate of evolving injury may influence the cell death cascade. Oxidative stress evolves acutely in ischemia-reperfusion injury, and the major morphology of neurodegeneration in selectively vulnerable regions is necrosis. In contrast, oxidative stress evolves slowly in axotomy/target deprivation, and the neurodegeneration resembles apoptosis. We have also identified that neuronal maturity and glutamate receptor subtypes can influence where a dying neuron falls along the cell death continuum. Neuronal apoptosis in the classic form may be more readily induced in the immature CNS after injury because activation of a PCD mechanism may be more accessible in immature neurons as compared to mature neurons. Conversely, some injured neurons in the adult CNS (as in geniculocortical neurons after target deprivation) may be less capable than immature neurons of showing a classic apoptotic morphology, and, therefore, their phenotype closely approximates but does not fully achieve the phenotype of classic apoptosis found during naturally occurring neuronal death in development.

Apoptotic and necrotic forms of cell death also coexist separately in different populations of cells following CNS injury, although they are probably not independent of each other. For example, global cerebral ischemia results in the primary degeneration of selectively vulnerable neurons (e.g., cerebellar Purkinje cells), which appears morphologically necrotic, and also results in the secondary degeneration target-deprived neurons (e.g., granule cells) and subsets of glial cells (e.g., oligodendrocytes), which is apoptotic. Therefore, a single insult to the CNS can cause death or injury to different populations of cells resulting from multiple, distinct causal processes that temporally overlap. The neuropathological outcome of CNS insults in animal models of excitoxicity, cerebral ischemia, target deprivation/axotomy, and in human neurological disorders is not likely to result from only a single process or causal mechanism (Fig. 16). The further exploration of these concepts may have fundamental importance with respect to how neurodegeneration is viewed in adult and pediatric neurological disorders.

ACKNOWLEDGMENTS

The authors are grateful for the expert technical assistance of Ann Price, Dawn Spicer, and Frank Barksdale. This work was supported by grants from the U.S. Public Health Service (NS34100 and NS20020) and the American Federation for Aging Research.

REFERENCES

1. Al-Abdulla, N. A.; Portera-Cailliau, C.; Martin, L. J. Occipital cortex ablation in adult rat causes retrograde neuronal death in the lateral geniculate nucleus that resembles apoptosis. Neuroscience, in press.
2. Al-Abdulla, N. A.; Martin, L. J. Apoptosis of retrogradely degenerating neurons occurs in association with the accumulation of perikaryal mitochondria and oxidative damage to the nucleus. Am. J. Pathol., in press.
3. Allen, T. D. Ultrastructural aspects of cell death. In: Potten, C. S., ed. Perspectives on mammalian cell death. New York: Oxford University Press; 1987:39–65.
4. Anderson, A. J.; Su, J. H.; Cotman, C. W. DNA damage and apoptosis in Alzheimer's disease: Colocalization with c-jun immunoreactivity, relationship to brain area, and effect of postmortem delay. J. Neurosci. 16:1710–1719; 1996.
5. Ankarcrona, M.; Dypbukt, J. M.; Bonfoco, E.; Zhivotovsky, B.; Orrenius, S.; Lipton, S. A.; Nicotera, P. Glutamate-induced neuronal death: A succession of necrosis or apoptosis depending on mitochondrial function. Neuron 15:961–973; 1995.
6. Antonsson, B.; Conti, F.; Ciavatta, A.; Montessuit, S.; Lewis, S.;

Martinou, I.; Bernasconi, L.; Bernard, A.; Mermod, J.-J.; Mazzei, G.; Maundrell, K., Gambale, F.; Sadoul, R.; Martinou, J.-C. Inhibition of bax channel-forming activity by bcl-2. Science 277:370–372; 1997.
7. Araki, T.; Kato, H.; Inoue, T.; Kogure, K. Regional impairment of protein synthesis following brief cerebral ischemia in the gerbil. Acta Neuropathol. 79:501–505; 1990.
8. Arends, M. J.; Morris, R. G.; Wyllie, A. H. Apoptosis. The role of endonuclease. Am. J. Pathol. 136:593–608; 1990.
9. Bansal, N.; Houle, A.; Melnykovych, G. Apoptosis: Mode of cell death induced in T cell leukemia lines by dexamethasone and other agents. FASEB J. 5:211–216; 1991.
10. Barinaga, M. Neurotrophic factors enter the clinic. Science 264:772–774; 1994.
11. Barron, K. D.; Means, E. D.; Larsen, E. Ultrastructure of retrograde degeneration in thalamus of rat. I. Neuronal somata and dendrites. J. Neuropathol. Exp. Neurol. 32:218–244; 1973.
12. Beilharz, E. J.; Williams, C. E.; Dragunow, M.; Sirimanne, E. S.; Gluckman, P. D. Mechanisms of delayed cell death following hypoxic-ischemic injury in the immature rat: Evidence for apoptosis during selective neuronal loss. Mol. Brain Res. 29:1–14; 1995.
13. Berkelaar, M.; Clarke, D. B.; Wang, Y.-C.; Bray, G. M.; Aguayo, A. J. Axotomy results in delayed death and apoptosis of retinal ganglion cells in adult rats. J. Neurosci. 14:4368–4374; 1994.
14. Bhat, R. V.; DiRocco, R.; Marcy, V. R.; Flood, D. G.; Zhu, Y.; Dobrzanski, P.; Siman, R.; Scott, R.; Contreras, P. C.; Miller, M. Increased expression of IL-1β converting enzyme in hippocampus after ischemia: Selective localization in microglia. J. Neurosci. 16: 4146–4154; 1996.
15. Bredesen, D. E. Neural apoptosis. Ann. Neurol. 38:839–851; 1995.
16. Brown, A. W.; Brierley, J. B. Anoxic-ischaemic cell change in rat brain: Light microscopic and fine-structural observations. J. Neurol. Sci. 16:59–84; 1972.
17. Bunch, S. T.; Fawcett, J. W. NMDA receptor blockade alters the topography of naturally ocurring ganglion cell death in rat retina. Dev. Biol. 160:434–442; 1993.
18. Bursch, W.; Paffe, S.; Putz, B.; Barthel, G.; Schulte-Hermann, R. Determination of the length of the histological stages of apoptosis in normal liver and in altered hepatic foci of rats. Carcinogenesis 11:847–853; 1990.
19. Catsicas, M.; Péquignot, Y.; Clarke, P. G. H. Rapid onset of neuronal death induced by blockade of either axoplasmic transport or action potentials in afferent fibers during brain development. J. Neurosci. 12:4642–4650; 1992.
20. Chen, J.; Graham, S. H.; Nakayama, M.; Zhu, R. L.; Jin, K.; Stetler, R. A.; Simon, R. P. Apoptosis repressor genes bcl-2 and bcl-x-long are expressed in the rat brain following global ischemia. J. Neurochem. 67:64–71; 1997.
21. Chen, J.; Zhu, R. L.; Nakayama, M.; Kawaguchi, K.; Jin, K.; Stetler, R. A.; Simon, R. P.; Graham, S. H. Expression of the apoptosis-effector gene, *bax*, is up-regulated in vulnerable hippocampal CA1 neurons following global ischemia. J. Neurochem. 67:64–71; 1996.
22. Choi, D. W. Excitotoxic cell death. J. Neurobiol. 23:1261–1276; 1992.
23. Chu-Wang, I.-W.; Oppenheim, R. W. Cell death of motoneurons in the chick embryo spinal cord. I. A light and electron microscopic study of naturally occurring and induced cell loss during development. J. Comp. Neurol. 177:33–58; 1978.
24. Clarke, P. G. H. Developmental cell death: Morphological diversity and multiple mechanisms. Anat. Embryol. 181:195–213; 1990.
25. Clarke, P. G. H.; Egloff, M. Combined effects of deafferentation and de-efferentation on isthmo-optic neurons during the period of their naturally occurring cell death. Anat. Embryol. 179:103–108; 1988.
26. Collins, R. J.; Harmon, B. V.; Gobé, V. C.; Kerr, J. F. R. Internucleosomal DNA clevage should not be the sole criterion for identifying apoptosis. Int. J. Radiat. Biol. 61:451–453; 1992.
27. Cooper, J. D.; Skepper, J. N.; da Penha Berzaghi, M.; Lindholm, D.; Sofroniew, M. V. Delayed death of septal cholinergic neurons after excitotoxic ablation of hippocampal neurons during early postnatal development in the rat. Exp. Neurol. 139:143–155; 1996.
28. Dean, R. T. Some critical membrane events during mammalian cell death. In: Potten, C. S., ed. Perspectives on mammalian cell death. New York: Oxford University Press; 1987:18–38.
29. Decker, R. S. Retrograde responses of developing lateral motor column neurons. J. Comp. Neurol. 180:635–660; 1978.
30. Deckwerth, T. L.; Elliott, J. L.; Knudson, C. M.; Johnson, E. M.; Snider, W. D.; Korsmeyer, S. J. Bax is required for neuronal death after trophic factor deprivation and during development. Neuron 17:401–411; 1996.
31. Deshmukh, M.; Vasilakos, J.; Deckwerth, T. L.; Lampe, P. A.; Shivers, B. D.; Johnson, E. M. Genetic and metabolic status of NGF-deprived sympathetic neurons saved by an inhibitor of ICE family proteases. J. Cell Biol. 135:1341–1354; 1996.
32. Deshpande, J.; Bergstedt, K.; Linden, T.; Kalimo, H.; Wieloch, T. Ultrastructural changes in the hippocampal CA1 region following transient cerebral ischemia: Evidence against programmed cell death. Exp. Brain Res. 88:91–105; 1992.
33. Dessi, F.; Charriaut-Marlangue, C.; Khrestchatisky, M.; Ben-Ari, Y. Glutamate-induced neuronal death is not a programmed cell death in cerebellar culture. J. Neurochem. 60:1953–1955; 1993.
34. Dubois-Dauphin, M.; Frankowski, H.; Tsujimoto, Y.; Huarte, J.; Martinou, J.-C. Neonatal motoneurons overexpressing the bcl-2 protooncogene in transgenic mice are protected from axotomy-induced cell death. Proc. Natl. Acad. Sci. USA 91:3309–3313; 1994.
35. Duke, R. C.; Chervenak, R.; Cohen, J. J. Endogeneous endonuclease-induced DNA fragmentation: An early event in cell-mediated cytolysis. Proc. Natl. Acad. Sci. USA 80:6361–6365; 1983.
36. Eriksson, N. P.; Lindsay, R. M.; Aldskogius, H. BDNF and NT-3 rescue sensory but not motoneurons following axotomy in the neonate. NeuroReport 5:1445–1448; 1994.
37. Ernfors, P.; Lee, K.-F.; Jaenisch, R. Mice lacking brain-derived neurotrophic factor develop with sensory deficits. Nature 368:147–150; 1994.
38. Farber, J. L.; Chien, K. R.; Mittnacht, S. The pathogenesis of irreversible cell injury in ischemia. Am. J. Pathol. 102:271–281; 1981.
39. Fariñas, I.; Jones, K. R.; Backus, C.; Wang, X.-Y.; Reichardt, L. F. Severe sensory and sympathetic deficits in mice lacking neurotrophin-3. Nature 369:658–661; 1994.
40. Farlie, P. G.; Dringen, R.; Rees, S. M.; Kannourakis, G.; Bernard, O. Bcl-2 transgene expression can protect neurons against developmental and induced cell death. Proc. Natl. Acad. Sci. USA 92:4397–4401; 1995.
41. Ferrer, I.; Martin, F.; Serrano, T.; Reiriz, J.; Pérez-Navarro, E.; Alberch, J.; Macaya, A.; Planas, A. M. Both apoptosis and necrosis occur following intrastriatal administration of excitotoxins. Acta Neuropathol. 90:504–510; 1995.
42. Fotuhi, M.; Dawson, T. M.; Sharp, A. H.; Martin, L. J.; Graybiel, A. M.; Snyder, S. H. Phosphoinositide second messenger system is enriched in striosomes: Immunohistochemical demonstration of inositol 1,4,5-trisphosphate receptors and phospholipase C β and γ in primate basal ganglia. J. Neurosci. 13:3300–3308; 1993.
43. Fry, F. J.; Cowan, W. M. A study of retrograde cell degeneration in the lateral mammillary nucleus of the cat, with special reference to the role of axonal branching in the preservation of the cell. J. Comp. Neurol. 144:1–24; 1972.
44. Fukuda, K.; Kojiro, M.; Chiu, J.-F. Demonstration of extensive chromatin cleavage in transplanted Morris hepatoma 7777 tissue: Apoptosis or necrosis? Am. J. Pathol. 142:935–946; 1993.
45. Furuta, S.; Ohta, S.; Hatakeyama, T.; Nakamura, K.; Sakaki, S. Recovery of protein synthesis in tolerance-induced hippocampal CA1 neurons after transient forebrain ischemia. Acta Neuropathol. 86: 329–336; 1993.
46. Gagliardini, V.; Fernandez, P.; Lee, R. K. K.; Drexler, H. C. A.; Rotello, R. J.; Fishman, M. C.; Yuan, J. Prevention of vertebrate neuronal death by crmA gene. Science 263:826–828; 1994.
47. Gavrieli, Y.; Sherman, Y.; Ben-Sasson, S. A. Identification of programmed cell death in situ via specific labeling of nuclear DNA fragmentation. J. Cell Biol. 119:493–501; 1992.
48. Gerschenson, L. E.; Rotello, R. J. Apoptosis: A different type of cell death. FASEB J. 6:2450–2455; 1992.
49. Ginsberg, S. D.; Martin, L. J. Ultrastructural analysis of the progression of neurodegeneration in the septum following fimbria-fornix transection. Neuroscience, in press.
50. Ginsberg, S. D.; Portera-Cailliau, C.; Martin, L. J. Fimbria-fornix

transection and excitotoxicity produce similar neurodegeneration in septum. Neuroscience, in press.
51. Giulian, D.; Vaca, K. Inflammatory glia mediate delayed neuronal damage after ischemia in the central nervous system. Stroke 24 [suppl I]:I84–I90; 1993.
52. Glücksmann, A. Cell deaths in normal vertebrate ontogeny. Biol. Rev. 26:59–86; 1951.
53. Gobé, G. C.; Axelsen, R. A.; Searle, J. W. Cellular events in experimental unilateral ischemic renal atrophy and in regeneration after contralateral nephrectomy. Lab. Invest. 63:770–779; 1990.
54. Gold, R.; Schmied, M.; Giegerich, G.; Breitschopf, H.; Hartung, H. P.; Toyka, K. V.; Lassmann, H. Differentiation between cellular apoptosis and necrosis by combined use of *in situ* tailing and nick translation techniques. Lab. Invest. 71:219–225; 1994.
55. Goto, K.; Ishige, A.; Sekiguchi, K.; Iizuka, S.; Sugimoto, A.; Yuzurihara, M.; Aburada, M.; Hosoya, E.; Kogure, K. Effects of cycloheximide on delayed neuronal death in rat hippocampus. Brain Res. 534:299–302; 1990.
56. Grasl-Kraupp, B.; Ruttkay-Nedecky, B.; Koudelka, H.; Bukowska, K.; Bursch, W.; Schulte-Hermann, R. *In situ* detection of fragmented DNA (TUNEL assay) fails to discriminate among apoptosis, necrosis, and autolytic cell death: A cautionary note. FASEB J. 21:1465–1468; 1995.
57. Greensmith, L.; Hasan, H. I.; Vrbová, G. Nerve injury increases the susceptibility of motoneurons to *N*-methyl-D-aspartate-induced neurotoxicity in the developing rat. Neuroscience 58:727–733; 1994.
58. Greensmith, L.; Vrbová, G. Motoneurone survival: A functional approach. Trends Neurosci. 19:450–455; 1996.
59. Gwag, B. J.; Koh, J. Y.; DeMaro, J. A.; Ying, H. S.; Jacquin, M.; Choi, D. W. Slowly triggered excitotoxicity occurs by necrosis in cortical cultures. Neuroscience 77:393–401; 1997.
60. Haas, C. A.; Deller, T.; Naumann, T.; Frotscher, M. Selective expression of the immediate early gene *c-jun* in axotomized rat medial septal neurons is not related to neuronal degeneration. J. Neurosci. 16:1894–1903; 1996.
61. Hamburger, V. Cell death in the development of the lateral motor column of the chick embryo. J. Comp. Neurol. 160:535–546; 1975.
62. Hamburger, V.; Levi-Montalcini, R. Proliferation, differentiation and degeneration in the spinal ganglia of the chick embryo under normal and experimental conditions. J. Exp. Zool. 111:457–501; 1949.
63. Hasegawa, Y.; Bonavida, B. Calcium-independent pathway of tumor necrosis factor-mediated lysis of target cells. J. Immunol. 142:2670–2676; 1989.
64. Heimer, L.; Kalil, R. Rapid transneuronal degeneration and death of cortical neurons following removal of the olfactory bulb. J. Comp. Neurol. 178:559–610; 1978.
65. Héron, A.; Pollard, H.; Dessi, F.; Moreau, J.; Lasbennes, F.; Ben-Ari, Y.; Charriaut-Marlangue, C. Regional variability in DNA fragmentation after global ischemia evidenced by combined histological and gel electrophoresis observations in the rat brain. J. Neurochem. 61:1973–1976; 1993.
66. Hill, I. E.; MacManus, J. P.; Rasquinha, I.; Tuor, U. I. DNA fragmentation indicative of apoptosis following unilateral cerebral hypoxia-ischemia in the neonatal rat. Brain Res. 676:398–403; 1995.
67. Hockenbery, D. M.; Oltvai, Z. N.; Yin, X.-M.; Milliman, C. L.; Korsmeyer, S. J. Bcl-2 functions in an antioxidant pathway to prevent apoptosis. Cell 75:241–251; 1993.
68. Hornung, J. P.; Koppel, H.; Clarke, P. G. H. Endocytosis and autophagy in dying neurons: An ultrastructural study in chick embryos. J. Comp. Neurol. 283:425–437; 1989.
69. Ito, U.; Spatz, M.; Walker, J. T.; Klatzo, I. Experimental cerebral ischemia in mongolian gerbils. I. Light microscopic observations. Acta Neuropathol. 32:209–223; 1975.
70. Iwasaki, Y.; Ikeda, K.; Shiojima, T.; Kinoshita, M. CNQX prevents spinal motor neuron death following sciatic nerve transection in newborn rats. J. Neurol. Sci. 134:21–25; 1995.
71. Iwata, M.; Hirano, A. Sparing of the Onufrowicz nucleus in sacral anterior horn lesions. Ann. Neurol. 4:245–249; 1978.
72. Jakowec, M. W.; Fox, A. J.; Martin, L. J.; Kalb, R. G. Quantitative and qualitative changes in AMPA receptor expression during spinal cord development. Neuroscience 67:893–907; 1995.
73. Johansen, F. F.; Diemer, N. H. Temporal profile of interneuron and pyramidal cell protein synthesis in rat hippocampus following cerebral ischemia. Acta Neuropathol. 81:14–19; 1990.
74. Jones, K. R.; Fariñas, I.; Backus, C.; Reichardt, L. F. Targeted disruption of the BDNF gene perturbs brain and sensory neuron development but not motor neuron development. Cell 76:989–999; 1994.
75. Kerr, J. F. R. An electron-microscopic study of liver cell necrosis due to heliotrine. J. Pathol. 97:557–562; 1969.
76. Kerr, J. F. R. Shrinkage necrosis: A distinct mode of cellular death. J. Pathol. 105:13–20; 1971.
77. Kerr, J. F. R.; Gobé, G. C.; Winterford, C. M.; Harmon, B. V. Anatomical methods in cell death. In: Schwartz, L. M.; Osborne, B. A., eds. Cell death. New York: Academic Press; 1995:1–27.
78. Kerr, J. F. R.; Harmon, B. V. Definition and incidence of apoptosis: An historical perspective. In: Tomei, L. D.; Cope, F. O., eds. Apoptosis: The molecular basis of cell death. Cold Spring Harbor, NY: Cold Spring Harbor Laboratory Press; 1991:5–29.
79. Kerr, J. F. R.; Searle, J. Deletion of cells by apoptosis during castration-induced involution of the rat prostate. Virchows Arch. Abt. B Zellpath. 13:87–102; 1973.
80. Kerr, J. F. R.; Wyllie, A. H.; Currie, A. R. Apoptosis: A basic biological phenomenon with wide-ranging implications in tissue kinetics. Br. J. Cancer 26:239–257; 1972.
81. Kirino, T. Delayed neuronal death in the gerbil hippocampus following ischemia. Brain Res. 239:57–69; 1982.
82. Kirino, T.; Sano, K. Fine structural nature of delayed neuronal death following ischemia in the gerbil hippocampus. Acta Neuropathol. 62:209–218; 1984.
83. Kirino, T.; Tamura, A.; Sano, K. Delayed neuronal death in rat hippocampus following transient forebrain ischemia. Acta Neuropathol. 64:139–147; 1984.
84. Kirsch, J. R.; Bhardwaj, A.; Martin, L. J.; Hanley, D. F.; Traystman, R. J. Neither L-arginine nor L-NAME affect neurological outcome after global ischemia in cats. Stroke 28:2259–2264; 1997.
85. Kitagawa, K.; Matsumoto, M.; Niinobe, M.; Mikoshiba, K.; Hata, R.; Ueda, H.; Handa, N.; Fukunaga, R.; Isaka, Y.; Kimura, K.; Kamada, T. Microtubule-associated protein 2 as a sensitive marker for cerebral ischemic damage. Immunohistochemical investigation of dendritic damage. Neuroscience 31:401–411; 1989.
86. Kluck, R. M.; Bossy-Wetzel, E.; Green, D. R.; Newmeyer, D. D. The release of cytochrome c from mitochondria: A primary site for bcl-2 regulation of apoptosis. Science 275:1132–1136; 1997.
87. Koh, J. Y.; Suh, S. W.; Gwag, B. J.; He, Y. Y.; Hsu, C. Y.; Choi, D. W. The role of zinc in selective neuronal death after transient global cerebral ischemia. Science 272:1013–1016; 1996.
88. Krajewski, S.; Mai, J. K.; Krajewska, M.; Sikorska, M.; Mossakowski, M. J.; Reed, J. C. Upregulation of bax protein levels in neurons following cerebral ischemia. J. Neurosci. 15:6364–6376; 1995.
89. Kroemer, G.; Petit, P.; Zamzami, N.; Vayssière, J.-L.; Mignotte, B. The biochemistry of programmed cell death. FASEB J. 9:1277–1287; 1995.
90. Kure, S.; Tominaga, T.; Yoshimoto, T.; Tada, K.; Narisawa, K. Glutamate triggers internucleosomal DNA cleavage in neuronal cells. Biochem. Biophys. Res. Commun. 179:39–45; 1991.
91. Laiho, K. U.; Shelburne, J. D.; Trump, B. J. Observations on cell volume, ultrastructure, mitochondrial conformation and vital-dye uptake in Ehrlich ascites tumor cells. Am. J. Pathol. 65:203–230; 1971.
92. Laiho, K. U.; Trump, B. J. Studies on the pathogenesis of cell injury. Effects of inhibitors of metabolism and membrane function on the mitochondria of Ehrlich ascites tumor cells. Lab. Invest. 32:163–182; 1975.
93. Lashley, K. S. The mechanism of vision. VIII. The projection of the retina upon the cerebral cortex. J. Comp. Neurol. 60:57–79; 1934.
94. Lashley, K. S. Thalamo-cortical connections of the rat's brain. J. Comp. Neurol. 75:67–121; 1941.
95. LaVelle, A.; LaVelle, F. W. The nucleolar apparatus and neuronal reactivity in injury during development. J. Exp. Zool. 137:285–315; 1958.
96. Lawrence, M. S.; Ho, D. Y.; Sun, G. H.; Steinberg, G. K.; Sopolsky, R. M. Overexpression of Bcl-2 with Herpes simplex virus vectors

protects CNS neurons against neurological insults *in vitro* and *in vivo*. J. Neurosci. 16:486–496; 1996.
97. Lefebvre, S.; Burglen, L.; Reboullet, S.; Clermont, O.; Burlet, P.; Viollet, L.; Benichou, B.; Cruaud, C.; Millasseau, P.; Zeviani, M.; Le Paslier, D.; Frezal, J.; Cohen, D.; Weissenbach, J.; Munnich, A.; Melki, J. Identification and characterization of a spinal muscular atrophy-determining gene. Cell 80:155–165; 1995.
98. Leppin, C.; Finiels-Marlier, F.; Crawley, J. N.; Montpied, P.; Paul, S. M. Failure of a protein synthesis inhibitor to modify glutamate receptor-mediated neurotoxicity in vivo. Brain Res. 581:168–170; 1992.
99. Li, P.; Nijhawan, D.; Budihardjo, I.; Srinivasula, S. M.; Ahmad, M.; Alnemri, E. S.; Wang, X. Cytochrome c and dATP-dependent formation of Apaf-1/caspase-9 complex initiates an apoptotic protease cascade. Cell 91:479–489; 1997.
100. Li, Y.; Sharov, V. G.; Jiang, N.; Zalago, C.; Sabbah, H. N.; Chopp, M. Ultrastructural and light microscopic evidence of apoptosis after middle cerebral artery occlusion in the rat. Am. J. Pathol. 146:1045–1051; 1995.
101. Lieberman, A. R. The axon reaction: A review of the principal features of perikaryal responses to axon injury. Int. Rev. Neurobiol. 14:49–124; 1971.
102. Linden, R. The survival of developing neurons: A review of afferent control. Neuroscience 58:671–682; 1994.
103. Linnik, M. D.; Zahos, P.; Geschwind, M. D.; Federoff, H. J. Expression of bcl-2 from a defective Herpes simplex virus-1 vector limits neuronal death in focal cerebral ischemia. Stroke 26:1670–1675; 1995.
104. Linnik, M. D.; Zobrist, R. H.; Hatfield, M. D. Evidence supporting a role for programmed cell death in focal cerebral ischemia in rats. Stroke 24:2002–2009; 1993.
105. Lipton, S. A.; Rosenberg, P. A. Excitatory amino acids as a final common pathway for neurologic disorders. N. Engl. J. Med. 330: 613–622; 1994.
106. Lithgow, T.; van Driel, R.; Bertram, J. F.; Strasser, A. The protein product of the oncogene *bcl-2* is a component of the nuclear envelope, the endoplasmic reticulum, and the outer mitochondrial membrane. Cell Growth Differ. 5:411–417; 1994.
107. Liu, X.; Ernfors, P.; Wu, H.; Jaenisch, R. Sensory but not motor neuron deficits in mice lacking NT4 and BDNF. Nature 375:238–241; 1995.
108. Liu, X.; Kim, C. N.; Yang, J.; Jemmerson, R.; Wang, X. Induction of apoptotic program in cell-free extracts: Requirement for dATP and cytochrome c. Cell 86:147–157; 1996.
109. Liu, X.; Zou, H.; Slaughter, C.; Wang, X. DFF, a heterodimeric protein that functions downstream of caspase-3 to trigger DNA fragmentation during apoptosis. Cell 89:175–184; 1997.
110. Lucas, D. R.; Newhouse, J. P. The toxic effect of sodium L-glutamate on the inner layers of the retina. Arch. Ophthal. 58:193–201; 1957.
111. Lucassen, P. J.; Chung, W. C. J.; Kamphorst, W.; Swaab, D. F. DNA damage distribution in the human brain as shown by in situ end labeling; area-specific differences in aging and Alzheimer's disease in the absence of apoptotic morphology. J. Neuropathol. Exp. Neurol. 56:887–900; 1997.
112. MacManus, J. P.; Hill, I. E.; Preston, E.; Rasquinha, I.; Walker, T.; Buchan, A. M. Differences in DNA fragmentation following transient cerebral ischemia or decapitation ischemia in rats. J. Cereb. Blood Flow Metabol. 15:728–737; 1995.
113. Majno, G.; Joris, I. Apoptosis, oncosis, and necrosis. An overview of cell death. Am. J. Pathol. 146:3–15; 1995.
114. Martin, L. J.; Blackstone, C. D.; Huganir, R. L.; Price, D. L. Cellular localization of a metabotropic glutamate receptor in rat brain. Neuron 9:259–270; 1992.
115. Martin, L. J.; Blackstone, C. D.; Huganir, R. L.; Price, D. L. The striatal mosaic in primates: Striosomes and matrix are differentially enriched in ionotropic glutamate receptor subunits. J. Neurosci. 13: 782–792; 1993.
116. Martin, L. J.; Blackstone, C. D.; Levey, A. I.; Huganir, R. L.; Price, D. L. AMPA glutamate receptor subunits are differentially distributed in rat brain. Neuroscience 53:327–358; 1993.
117. Martin, L. J.; Brambrink, A.; Koehler, R. C.; Traystman, R. J. Primary sensory and forebrain motor systems in the newborn brain are preferentially damaged by hypoxia-ischemia. J. Comp. Neurol. 377:262–285; 1997.
118. Martin, L. J.; Brambrink, A.; Koehler, R. C.; Traystman, R. J. Neonatal asphyxic brain injury is neural system preferential and targets sensory-motor networks. In: Stevenson, D. K.; Sunshine, P., eds. Fetal and neonatal brain injury: Mechanisms, management, and the risks of practice. New York: Oxford University Press; 1997:374–399.
119. Martin, L. J.; Brambrink, A. M.; Ichord, R. N.; Portera-Cailliau, C.; Northington, F. J.; Koehler, R. C.; Traystman, R. J. Hypoxia-ischemia in newborns causes nonapoptotic striatal neuron death that evolves with transient mitochondrial activation, increased protein phosphorylation, oxidative injury, and early damage to the golgi. Soc. Neurosci. Abstr. 23:2186; 1997.
120. Martin, L. J.; Brambrink, A. M.; Lehmann, C.; Portera-Cailliau, C.; Koehler, R.; Rothstein, J.; Traystman, R. J. Hypoxia-ischemia causes abnormalities in glutamate transporters and death of astroglia and neurons in newborn striatum. Ann. Neurol. 42:335–348; 1997.
121. Martin, L. J.; Doebler, J. A.; Shih, T.; Anthony, A. Cytophotometric analyses of thalamic neuronal RNA in soman intoxicated rats. Life Sci. 35:1593–1600; 1984.
122. Martin, L. J.; Doebler, J. A.; Swisher, J. W.; Shih, T.; Anthony, A. Scanning cytophotometric analysis of myocardial nucleic acid and chromatin changes in soman toxicated rabbits. Cell Biochem. Funct. 2:237–242; 1984.
123. Martinou, J.-C.; Dubois-Dauphin, M.; Staple, J. K.; Rodriguez, I.; Frankowski, H.; Missotten, M.; Albertini, P.; Talabot, D.; Catsicas, S.; Pietra, C.; Huarte, J. Overexpression of bcl-2 in transgenic mice protects neurons from naturally occurring cell death and experimental ischemia. Neuron 13:1017–1030; 1994.
124. Masu, Y.; Wolf, E.; Holtmann, B.; Sendtner, M.; Brem, G.; Thoenen, H. Distruption of the CNTF gene results in motor neuron degeneration. Nature 365:27–32; 1993.
125. Matsuo, Y.; Onodera, H.; Shiga, Y.; Nakamura, M.; Ninomiya, M.; Kihara, T.; Kogure, K. Correlation between myeloperoxidase-quantified neurtophil accumulation and ischemic brain injury in the rat. Effects of neutrophil depletion. Stroke 25:1469–1475; 1994.
126. Matter, A. Microcinematographic and electron microscopic analysis of target cell lysis induced by cytotoxic T lymphocytes. Immunology 36:179–190; 1979.
127. Matthews, M. A. Death of the central neuron: An electron microscopic study of thalamic retrograde degeneration following cortical ablation. J. Neurocytol. 2:265–288; 1973.
128. Mehmet, H.; Yue, X.; Squier, M. V.; Lorek, A.; Cady, E.; Penrice, J.; Sarraf, C.; Wylezinska, M.; Kirkbride, V.; Cooper, C.; Brown, G. C.; Wyatt, J. S.; Reynolds, E. O. R.; Edwards, A. D. Increased apoptosis in the cingulate sulcus of newborn piglets following transient hypoxia-ischaemia is related to the degree of high energy phosphate depletion during the insult. Neurosci. Lett. 181:121–125; 1994.
129. Mentis, G. Z.; Greensmith, L.; Vrbová, G. Motoneurons destined to die are rescued by blocking *N*-methyl-D-aspartate receptors by MK-801. Neuroscience 54:283–285; 1993.
130. Mergner, W. J.; Jones, R. T.; Trump, B. J. Cell death: Mechanisms of acute and lethal cell injury. New York: Field & Wood; 1990.
131. Merry, D. E.; Korsmeyer, S. J. Bcl-2 gene family in the nervous system. Ann. Rev. Neurosci. 20:245–267; 1997.
132. Michaelidis, T. M.; Sendtner, M.; Cooper, J. D.; Airaksinen, M. S.; Holtmann, B.; Meyer, M.; Thoenen, H. Inactivation of bcl-2 results in progressive degeneration of motoneurons, sympathetic and sensory neurons during early postnatal development. Neuron 17:75–89; 1996.
133. Migheli, A.; Cavalla, P.; Marino, S.; Schiffer, D. A study of apoptosis in normal and pathologic nervous tissue after in situ end-labeling of DNA strand breaks. J. Neuropathol. Exp. Neurol. 53:606–616; 1994.
134. Milligan, C. E.; Prevette, D.; Yaginuma, H.; Homma, S.; Cardwell, C.; Fritz, L. C.; Tomaselli, K. J.; Oppenheim, R. W.; Schwartz, L. M. Peptide inhibitors of the ICE protease family arrest programmed cell death of motoneurons in vivo and in vitro. Neuron 15:385–393; 1995.
135. Mirabelli, F.; Salis, A.; Marinoni, V.; Finardi, G.; Bellomo, G.; Thor, H.; Orrenius, S. Menadione-induced bleb formation in hepatocytes is associated with the oxidation of thiol groups in actin. Biochem. Pharmacol. 37:3423–3427; 1988.

136. Mirabelli, F.; Salis, A.; Perotti, M.; Taddei, F.; Bellomo, G.; Orrenius, S. Alterations of surface morphology caused by the metabolism of menadione in mammalian cells are associated with the oxidation of critical sulfhydryl groups in cytoskeletal proteins. Biochem. Pharmacol. 37:3423–3427; 1988.
137. Mu, X.; He, J.; Anderson, D. W.; Trojanowski, J. Q.; Springer, J. E. Altered expression of *bcl-2* and *bax* mRNA in amyotrophic lateral sclerosis spinal cord motor neurons. Ann. Neurol. 40:379–386; 1996.
138. Naumann, T.; Peterson, G. M.; Frotscher, M. Fine structure of rat septohippocampal neurons: A time course analysis following axotomy. J. Comp. Neurol. 325:219–242; 1992.
139. Newmeyer, D. D.; Farschon, D. M.; Reed, J. C. Cell-free apoptosis in Xenopus egg extracts: Inhibition by bcl-2 and requirement for an organelle fraction enriched in mitochondria. Cell 79:353–364; 1994.
140. Nitatori, T.; Sato, N.; Waguri, S.; Karasawa, Y.; Araki, H.; Shibanai, K.; Kominami, E.; Uchiyama, Y. Delayed neuronal death in the CA1 pyramidal cell layer of the gerbil hippocampus following transient ischemia is apoptosis. J. Neurosci. 15:1001–1011; 1995.
141. O'Connor, T. M.; Wyttenbach, C. R. Cell death in the embryonic chick spinal cord. J. Cell Biol. 60:448–459; 1974.
142. Oberhammer, F.; Bursch, W.; Parzefall, W.; Breit, P.; Erber, E.; Stadler, M.; Schulte-Hermann, R. Effect of transforming growth factor β on cell death of cultured rat hepatocytes. Cancer Res. 51:2478–2485; 1991.
143. Oberhammer, F.; Fritsch, G.; Schmied, M.; Pavelka, M.; Printz, D.; Purchio, T.; Lassmann, H.; Schulte-Hermann, R. Condensation of the chromatin at the membrane of an apoptotic nucleus is not associated with activation of an endonuclease. J. Cell Sci. 104:317–326; 1993.
144. Okamoto, M.; Matsumoto, M.; Ohtsuki, T.; Taguchi, A.; Mikoshiba, K.; Yanagihara, T.; Kamada, T. Internucleosomal DNA cleavage involved in ischemia-induced neuronal death. Biochem. Biophys. Res. Commun. 196:1356–1362; 1993.
145. Olney, J. W. Glutamate-induced neuronal necrosis in the infant mouse hypothalamus. An electron microscopic study. J. Neuropathol. Exp. Neurol. 30:75–90; 1971.
146. Olney, J. W.; Rhee, V.; Ho, O. L. Kainic acid: A powerful neurotoxic analogue of glutamate. Brain Res. 77:507–512; 1974.
147. Oppenheim, R. W. Cell death during development of the nervous system. Ann. Rev. Neurosci. 14:453–501; 1991.
148. Peterson, G. M.; Naumann, T.; Frotscher, M. Identified septohippocampal neurons survive axotomy: A fine-structural analysis in the rat. Neurosci. Lett. 138:81–85; 1992.
149. Petito, C. K.; Pulsinelli, W. A. Sequential development of reversible and irreversible neuronal damage following cerebral ischemia. J. Neuropathol. Exp. Neurol. 43:141–153; 1984.
150. Pilar, G.; Landmesser, L. Ultrastructural differences during embryonic cell death in normal and peripherally deprived ciliary ganglia. J. Cell Biol. 68:339–356; 1976.
151. Pittman, R. N.; Wang, S.; DiBenedetto, A. J.; Mills, J. C. A system for characterizing cellular and molecular events in programmed neuronal cell death. J. Neurosci. 13:3669–3680; 1993.
152. Portera-Cailliau, C.; Price, D. L.; Martin, L. J. Non-NMDA and NMDA receptor-mediated excitotoxic neuronal deaths in adult brain are morphologically distinct: Further evidence for an apoptosis-necrosis continuum. J. Comp. Neurol. 378:88–104; 1997.
153. Portera-Cailliau, C.; Price, D. L.; Martin, L. J. Excitotoxic neuronal death in the immature brain is an apoptosis-necrosis morphological continuum. J. Comp. Neurol. 378:70–87; 1997.
154. Prestige, M. Differentiation, degeneration, and the role of the periphery: Quantitative considerations. In: Schmitt, F. O., ed. The neurosciences: Second study program. New York: Rockefeller University Press; 1970:73–82.
155. Price, D. L.; Martin, L. J.; Clatterbuck, R. E.; Koliatsos, V. E.; Sisodia, S. S.; Walker, L. C.; Cork, L. C. Neuronal degeneration in human diseases and animal models. J. Neurobiol. 23:1277–1294; 1992.
156. Przywara, D. A.; Bhave, S. V.; Bhave, A.; Wakade, T. D.; Wakade, A. R. Stimulated rise in neuronal calcium is faster and greater in the nucleus than the cytosol. FASEB J. 5:217–222; 1991.
157. Pulsinelli, W. A.; Brierley, J. B.; Plum, F. Temporal profile of neuronal damage in a model of transient forebrain ischemia. Ann. Neurol. 11:491–498; 1982.
158. Quigley, H. A.; Nickells, R. W.; Kerrigan, L. A.; Pease, M. E.; Thibault, D. J.; Zack, D. J. Retinal ganglion cell death in experimental glaucoma and after axotomy occurs by apoptosis. Invest. Ophthalmol. Vis. Sci. 36:774–786; 1995.
159. Ratan, R. R.; Murphy, T. H.; Baraban, J. M. Oxidative stress induces apoptosis in embryonic cortical cultures. J. Neurochem. 62:376–379; 1994.
160. Romanes, G. J. Motor localization and the effects of nerve injury on the ventral horn cells of the spinal cord. J. Anat. 80:117–131; 1946.
161. Roy, N.; Mahadevan, M. S.; McLean, M.; Shutler, G.; Yaraghi, Z.; Farahani, R.; Baird, S.; Besner-Johnston, A.; Lefebvre, C.; Kang, X.; Salih, M.; Aubry, H.; Tamai, K.; Guan, X.; Ioannou, P.; Crawford, T. O.; de Jong, P. J.; Surh, L.; Ikeda, J.-E.; Korneluk, R. G.; Mackenzie, A. The gene for neuronal apoptosis inhibitory protein is partially deleted in individuals with spinal muscular atrophy. Cell 80:167–178; 1995.
162. Russell, S. W.; Rosenau, W.; Lee, J. C. Cytolysis induced by human lymphotoxin. Cinemicrographic and electron microscopic observations. Am. J. Pathol. 69:103–118; 1972.
163. Saunders, J. W. Death in embryonic systems. Science 154:604–612; 1966.
164. Schreiber, S. S.; Tocco, G.; Najm, I.; Thompson, R. F.; Baudry, M. Cycloheximide prevents kainate-induced neuronal death and c-fos expression in adult rat brain. J. Mol. Neurosci. 4:149–159; 1993.
165. Schwartz, L. M.; Milligan, C. E. Cold thoughts of death: The role of ICE proteases in neuronal cell death. Trends Neurosci. 19:555–562; 1996.
166. Schwartz, L. M.; Smith, S. W.; Jones, M. E. E.; Osborne, B. A. Do all programmed cell deaths occur via apoptosis? Proc. Natl. Acad. Sci. USA 90:980–984; 1993.
167. Schweichel, J. U.; Merker, H. J. The morphology of various types of cell death in prenatal tissues. Teratology 7:253–266; 1973.
168. Sen, S. Programmed cell death: Concept, mechanism and control. Biol. Rev. 67:287–319; 1992.
169. Shi, Y.; Sahai, B. M.; Green, D. R. Cyclosporin A inhibits activation-induced cell death in T-cell hybridomas and thymocytes. Nature 339:625–626; 1989.
170. Shigeno, T.; Yamasaki, Y.; Kato, G.; Kusaka, K.; Mima, T.; Takakura, K.; Graham, D. I.; Furukawa, S. Reduction of delayed neuronal death by inhibition of protein synthesis. Neurosci. Lett. 120:117–119; 1990.
171. Sieber, F. E.; Palmon, S. C.; Traystman, R. J.; Martin, L. J. Global incomplete cerebral ischemia produces predominantly cortical neuronal injury. Stroke 26:2091–2096; 1995.
172. Sieber, F. E.; Traystman, R. J.; Martin, L. J. Delayed neuronal death after global incomplete ischemia in dogs is accompanied by changes in phospholipase C protein expression. J. Cereb. Blood Flow Metabol. 17:527–533; 1997.
173. Siman, R.; Noszek, J. C.; Kegerise, C. Calpain I activation is specifically related to excitatory amino acid induction of hippocampal damage. J. Neurosci. 9:1579–1590; 1989.
174. Simonian, N. A.; Getz, R. L.; Leveque, J. C.; Konradi, C.; Coyle, J. T. Kainate induces apoptosis in neurons. Neuroscience 74:675–683; 1996.
175. Sloviter, R. S.; Dean, E.; Neubort, S. Electron microscopic analysis of adrenalectomy-induced hippocampal granule cell degeneration in the rat: Apoptosis in the adult central nervous system. J. Comp. Neurol. 330:337–351; 1993.
176. Thilmann, R.; Xie, Y.; Kleihues, P.; Kiessling, M. Persistent inhibition of protein synthesis precedes delayed neuronal death in postischemic gerbil hippocampus. Acta Neuropathol. 71:88–93; 1986.
177. Tomei, L. D.; Shapiro, J. P.; Cope, F. O. Apoptosis in C3H/10T$^{1/2}$ mouse embryonic cells: Evidence for internucleosomal DNA modification in the absence of double-strand cleavage. Proc. Natl. Acad. Sci. USA 90:853–857; 1993.
178. Tominaga, T.; Kure, S.; Narisawa, K.; Yoshimoto, T. Endonuclease activation following focal ischemic injury in the rat brain. Brain Res. 608:21–26; 1993.
179. Torvik, A. Central chromatolysis and the axon reaction. A reappraisal. Neuropathol. Appl. Neurobiol. 2:423–432; 1976.
180. Torvik, A.; Heding, A. Effect of actinomycin D on retrograde nerve

cell reaction. Further observations. Acta Neuropathol. 14:62–71; 1969.
181. Torvik, A.; Skjörten, F. Electron microscopic observations on nerve cell regeneration and degeneration after axon lesions. I. Changes in the nerve cell cytoplasm. Acta Neuropathol. 17:248–264; 1971.
182. Troost, D.; Aten, J.; Morsink, F.; de Jong, J. M. B. V. Apoptosis in amyotrophic lateral sclerosis is not restricted to motor neurons. Bcl-2 expression is increased in unaffected post-central gyrus. Neuropath. Appl. Neurobiol. 21:498–504; 1995.
183. Trump, B. J.; Goldblatt, P. J.; Stowell, R. E. Studies on necrosis of mouse liver in vitro. Ultrastructural alterations in the mitochondria of hepatic parenchymal cells. Lab. Invest. 14:343–371; 1965.
184. Trump, B. J.; Goldblatt, P. J.; Stowell, R. E. Studies of mouse liver necrosis in vitro. Ultrastructural and cytochemical alterations in hepatic parenchymal cell nuclei. Lab. Invest. 14:1969–1999; 1965.
185. Vander Heiden, M. G.; Chandel, N. S.; Williamson, E. K.; Schumacker, P. T.; Thompson, C. B. Bcl-x_L regulates the membrane potential and volume homeostasis of mitochondria. Cell 91:627–637; 1997.
186. van Lookeren Campagne, M.; Lucassen, P. J.; Vermeulen, J. P.; Balázs, R. NMDA and kainate induced internucleosomal DNA cleavage associated with both apoptotic and necrotic cell death in the neonatal rat brain. Eur. J. Neurosci 7:1627–1640; 1995.
187. Vejsada, R.; Sagot, Y.; Kato, A. C. Quantitative comparison of the transient rescue effects of neurotrophic factors on axotomized motoneurons in vivo. Eur. J. Neurosci. 7:108–115; 1994.
188. Virchow, R. Cellular pathology as based upon physiological and pathological histology. London: Churchill; 1858.
189. Waring, P. DNA fragmentation induced in macrophages by gliotoxin does not require protein synthesis and is preceded by raised inositol triphosphate levels. J. Biol. Chem. 265:14476–14480; 1990.
190. Whetsell, W. O. Current concepts of excitotoxicity. J. Neuropathol. Exp. Neurol. 55:1–13; 1996.
191. Wong-Riley, M. T. T. Changes in the dorsal lateral geniculate nucleus of squirrel monkey after unilateral ablation of the visual cortex. J. Comp. Neurol. 146:519–548; 1972.
192. Wood, K. A.; Dipasquale, B.; Youle, R. J. In situ labeling of granule cells for apoptosis-associated DNA fragmentation reveals different mechanisms of cell loss in developing cerebellum. Neuron 11:621–632; 1993.
193. Wyllie, A. H. Glucocorticoid-induced thymocyte apoptosis is associated with enodgenous endonuclease activation. Nature 284:555–556; 1980.
194. Wyllie, A. H.; Kerr, J. F. R.; Currie, A. R. Cell death: The significance of apoptosis. Int. Rev. Cytol. 68:251–306; 1980.
195. Yamamoto, K.; Hayakawa, T.; Mogami, H.; Akai, F.; Yanagihara, T. Ultrastructural investigation of the CA1 region of the hippocampus after transient cerebral ischemia in gerbils. Acta Neuropathol. 80: 487–492; 1990.
196. Yang, J.; Liu, X.; Bhalla, K.; Kim, C. N.; Ibrado, A. M.; Cai, J.; Peng, T.-I.; Jones, D. P.; Wang, X. Prevention of apoptosis by bcl-2: Release of cytochrome c from mitochondria blocked. Science 275: 1129–1132; 1997.
197. Yoshiyama, Y.; Yamada, T.; Asanuma, K.; Asahi, T. Apoptosis related antigen, Le^Y and nick-end labeling are positive in spinal motor neurons in amyotrophic lateral sclerosis. Acta Neuropathol. 88:207–211; 1994.
198. Zamzami, N.; Susin, S. A.; Marchetti, P.; Hirsch, T.; Gómez-Monterrey, I.; Castedo, M.; Kroemer, G. Mitochondrial control of nuclear apoptosis. J. Exp. Med. 183:1533–1544; 1996.